

Monetary Policy Identification and Transmission: A Narrative High-Frequency Approach^{*}

Brian Amorim Cabaço[†] and Adriana Grasso[‡]

[Click here for the latest version](#)

November 5, 2025

Abstract

We identify four dimensions of monetary policy in the euro area using narrative restrictions applied to high-frequency data. By leveraging well-known historical episodes—such as Mario Draghi’s “whatever it takes” speech—we can separately identify conventional policy, forward guidance, quantitative easing, and asymmetric country risk premia shocks using a single narrative restriction per shock. After controlling for predictability in high-frequency asset movements and state-dependent variance in a Bayesian factor model, we find limited evidence for the importance of information shocks. We then use our shock measures to estimate the aggregate effects of monetary policy instruments. We implement a Bayesian VAR with distributed lags and stochastic volatility that allows for overidentifying restrictions on the impulse responses. We find that tightening along any monetary policy dimension causes declines in activity and inflation, though magnitudes vary considerably. Forward guidance has marginal effects on economic variables, while asset purchases induce larger impacts, but both remain less potent than conventional policy.

JEL Classification: E52, E58, E43, E44, C11, C32, C54

Keywords: monetary policy, high-frequency identification, forward guidance, quantitative easing, narrative restrictions, euro area

*We thank seminar participants at the ECB DG Monetary Policy and at the Surrey-UCL-Essex-Southampton Workshop in Macroeconomics for helpful comments and suggestions. The views expressed in this paper are those of the authors and do not necessarily reflect those of the European Central Bank. All errors are our own.

[†]University College London (UCL). Email: brian.cabaco.17@ucl.ac.uk.

[‡]European Central Bank (ECB). Email: adriana.grasso@ecb.europa.eu.

1 Introduction

Following the Great Recession, central banks across advanced economies have experimented with new unconventional monetary policy instruments to stimulate economic activity and achieve their inflation targets at the zero lower bound. Given the recency of these policies, there remains limited direct empirical evidence on the impact these measures have had on economic aggregates.

In this paper, we identify four dimensions of monetary policy using narrative restrictions and high-frequency data ([Kuttner, 2001](#); [Gürkaynak et al., 2005](#)) for the euro area. We use the identified shocks to estimate the aggregate dynamic causal effects of different monetary policy instruments. We find that contractionary shocks along any dimension induce persistent declines in economic activity and inflation, though conventional policy generates the largest responses.

Identification relies on well-known historical episodes during which one can mostly attribute asset price movements to a specific monetary policy instrument. For instance, during the January 22, 2015 Governing Council (GC) meeting, the European Central Bank (ECB) surprised markets by announcing a larger than expected asset purchase program, and long-dated yields fell sharply. We identify similar episodes for conventional monetary policy, forward guidance, quantitative easing, and asymmetric country risk premia. A single narrative sign restriction per shock is sufficient to tightly identify each shock separately.

We establish that for the euro area information shocks ([Nakamura and Steinsson, 2018](#); [Jarociński and Karadi, 2020](#)) play a negligible role in the high-frequency movements of assets around policy events. After controlling for predictability in high-frequency movements ([Bauer and Swanson , 2023](#)), four types of monetary policy shocks, and state-dependent variance in both policy shocks and idiosyncratic errors, we find there is very little residual variation left for information shocks to be meaningful. We show that, unlike the other monetary policy shocks we identify, the information shocks are noisy, do not display heavy-tails nor time-varying volatility, and are very difficult to tie to the historical record.

At the aggregate level, we propose to estimate the effects of monetary policy using a Bayesian VAR model with distributed lags (VAR-DL) for the policy shocks. This spec-

ification carries several advantages. First, distributed lag models are equivalent to local projections in terms of bias (Baek and Lee, 2022; Montiel Olea et al., 2025). Second, VAR-DL models are straightforward to estimate in a Bayesian setting.¹, which allows one to place overidentifying zero, sign, and magnitude restrictions on the impulse-responses. Third, Bayesian methods allow us to sample the monetary policy shocks from their high-frequency posterior at each MCMC iteration, thus naturally propagating estimation uncertainty from the high-frequency factor model to the aggregate impulse response estimates. Finally, we propose priors on the distributed lag coefficients which allow one to effectively trade off bias for variance by either penalizing the differences in adjacent impulse-response estimates or shrinking the entire impulse-response toward a low-order polynomial.

Our estimates indicate that forward guidance has small effects on economic activity, while the effects of quantitative easing are slightly smaller than those of conventional monetary policy. We find that a tightening along any of the monetary dimensions we consider causes declines in economic activity, prices, and in money supply. Importantly, the responses to forward guidance shocks exhibit puzzling behaviors when relying solely on high-frequency identification, with industrial production rising following a contractionary shock, thus contradicting standard theory. Imposing overidentifying dynamic sign restrictions eliminates these puzzles and produces theoretically consistent responses, suggesting that high-frequency instruments alone may be insufficient to cleanly identify the effects of forward guidance shocks. For asymmetric country risk premia shocks, we find evidence of stagflationary dynamics, with peripheral yields increasing very persistently over the entire forecast horizon, measures of economic activity weakening, and prices rising. The inflationary pressures stem from currency depreciation driven by heightened fragmentation risks.

Related Literature. This paper contributes to three main strands of the monetary policy literature: the high-frequency identification of monetary policy shocks, narrative identification approaches, and the estimation of the macroeconomic effects of monetary policy.

A large literature dating back to Kuttner (2001) and Gürkaynak et al. (2005) uses high-frequency asset price movements around policy announcements to identify monetary policy

¹On the other hand, local projections do not induce a proper likelihood and require Bayesian quasi-likelihood techniques, see Ferreira et al. (2025).

shocks. This approach exploits the idea that asset price changes in narrow windows around central bank communications primarily reflect news about monetary policy rather than other sources of macroeconomic fluctuations. [Swanson \(2021\)](#) extended earlier studies by identifying forward guidance and large-scale asset purchases shocks using exclusion restrictions that specify which assets can respond to each shock. [Altavilla et al. \(2019\)](#) employ similar methods for the euro area, but identify instead two dimensions of forward guidance. As in this paper, [Ricco et al. \(2025\)](#) also consider unconventional policy instruments, asymmetric risk country premia, and information shocks in the Euro area, but rely instead on exclusion restrictions as in [Altavilla et al. \(2019\)](#) and [Swanson \(2021\)](#).

Another strand of the literature identifies monetary policy shocks using narrative evidence from policy documents and historical records. [Romer and Romer \(1989\)](#) and [Romer and Romer \(2004\)](#) pioneered this approach by reading FOMC minutes to identify episodes during which the Federal Reserve exogenously tightened policy. [Cloyne and Hürtgen \(2016\)](#) apply similar methods to the United Kingdom. [Antolín-Díaz and Rubio-Ramírez \(2018\)](#) formalize the use of narrative restrictions in structural vector autoregression models with sign restrictions imposed on historical decompositions. [Badinger and Schiman \(2023\)](#) rely on that approach to identify the effects of conventional monetary policy shocks in the Euro area.

We contribute to these two strands of the literature by combining both high-frequency data with narrative restrictions to identify multiple dimensions of monetary policy. We employ a Bayesian factor model with regime-switching volatility in the structural shocks and idiosyncratic errors, capturing the characteristic pattern whereby extended periods of tranquility are punctuated by episodes of heightened policy activity. We show that a single narrative restriction per shock is sufficient to recover that shock without having to resort to exclusion restrictions, and that our shocks align closely with the historical record.

More recently, several studies have documented that monetary policy announcements convey information about the central bank's assessment of the economic outlook, prompting financial market responses beyond those attributable to policy changes alone ([Campbell et al., 2012](#); [Nakamura and Steinsson, 2018](#)). Using sign restrictions to separately identify conventional policy and information shocks, [Jarociński and Karadi \(2020\)](#) show that information

shocks associated with a rise in yields lead to increases in economic activity and prices. Using high-frequency data for the euro area, [Andrade and Ferroni \(2021\)](#) identify conventional monetary policy, Delphic (news) forward guidance, and Odyssean (policy) forward guidance shocks, and they obtain impulse responses similar to those reported by [Jarociński and Karadi \(2020\)](#).

The view that monetary policy announcements induce large reappraisals of the economic outlook by market participants has recently been challenged by ([Bauer and Swanson , 2023](#)). The authors show that high-frequency asset movements around central bank announcements are predictable, that surveyed professional forecasters do not revise their economic projections in a way that is consistent with the existence of information shocks, and that the forecasts made by the Federal Reserve are not more accurate than their private sector counterparts. They suggest instead that market participants underestimate the extent to which central banks respond to recent economic and financial developments, a channel they call "response to news". Both [Cieslak \(2018\)](#) and [Schmeling et al. \(2022\)](#) provide supporting empirical evidence that show markets fail to anticipate the scale of central banks' responses to large and infrequent shocks. Additionally, [Miranda-Agrippino and Ricco \(2021\)](#) document that controlling for predictability in high-frequency asset movements helps to reduce the puzzles encountered when using such instruments in monthly vector autoregressions, findings confirmed by both [Swanson \(2024\)](#) and [Ricco et al. \(2025\)](#).

We contribute to this debate in several ways. First, we develop a high-frequency Bayesian factor model which directly accounts for predictability in high-frequency asset price movements and models time-varying volatility in the monetary policy shocks and the idiosyncratic residuals. We find that neither the narrative nor the statistical evidence supports the existence of meaningful information effects. For the former, we fail to map the identified information shocks to policy events which conveyed material reassessments of the economic outlook by the ECB. For the latter, we show that information shocks do not display the heavy tails nor the time-varying heteroskedasticity characteristic of the other policy shocks we identify. At the same time, we find that both a composite index of systemic stress ([Hollo et al., 2012](#)) and an indicator of monetary policy uncertainty² ([Bauer et al., 2021](#)) are sig-

²We thank colleagues at the ECB for sharing this series for the euro area with us.

nificant predictors of high-frequency movements in yields with maturities of two years and greater.

Several papers have employed high-frequency monetary policy shocks to study the aggregate dynamic causal effects of monetary policy. Both [Gertler and Karadi \(2015\)](#) and [Caldara and Herbst \(2019\)](#) document the effects of conventional monetary policy shocks using high-frequency surprises as external instruments in a proxy-SVAR ([Mertens and Ravn, 2013](#); [Stock and Watson, 2012](#)). [Swanson \(2024\)](#) uses high-frequency surprises to estimate the effects of conventional policy, forward guidance, and large-scale asset purchases on US economic outcomes, and finds that conventional policy has the largest effects, while [Ricco et al. \(2025\)](#) perform a similar exercise for the Euro area.

We contribute to this literature in several ways. On the methodological side, we propose a Bayesian VAR with distributed lags (VAR-DL) that allows for overidentifying zero, sign, and magnitude restrictions on the impulse-responses. Distributed lag models deliver asymptotically unbiased impulse-responses up to the horizon of the distributed lag ([Baek and Lee, 2022](#); [Montiel Olea et al., 2025](#)). The Bayesian framework allows us to naturally propagate the uncertainty from the high-frequency shock identification stage to the macroeconomic analysis, whereas most of the prior literature treats the proxies as data. We develop flexible priors that penalize differences in adjacent impulse-response coefficients to impose smoothness, thereby substantially reducing the jaggedness characteristic of distributed lag and local projections impulse-response estimators while introducing minimal bias.

On the substantive side, we show that conventional policy remains the most effective instrument to achieve the ECB’s inflation mandate. We document that forward guidance shocks exhibit puzzling macroeconomic responses when relying on high-frequency identification only, consistent with findings by [Miranda-Agrippino and Ricco \(2023\)](#), [Swanson \(2024\)](#), and [Ricco et al. \(2025\)](#). Imposing theory-consistent and overidentifying dynamic sign restrictions resolves these puzzles. Finally, we show that adverse asymmetric country risk premia shocks generate stagflationary dynamics that contrast with the disinflationary effects generated by other policy instruments.

The rest of the paper is organized as follows. Section 2 describes the high-frequency Bayesian factor model and the identification strategy. Section 3 presents the identified

high-frequency monetary policy shocks and discusses the role played by information effects. Section 4 presents the Bayesian VAR-DL framework and estimates of the macroeconomic effects of different monetary policy instruments. Finally, section 5 concludes and discusses implications for monetary policy design in the euro area.

2 High-Frequency Identification

In this section, we describe the Bayesian factor model we use to identify high-frequency monetary policy surprises. We discuss the econometric implementation of our identification strategy and the identifying assumptions we rely upon.

2.1 Data and High-Frequency Model

The high-frequency analysis leverages the euro area Communication Event-Study Database (EA-CED) collected by [Istrefi et al. \(2024\)](#). The dataset covers the period 1999-2024 and includes high-frequency movements for overnight interest swaps (OIS), sovereign yields, exchange rates, stock price indices, and inflation-linked swaps (ILS) over 300 scheduled GC meetings and 4,400 intermeeting communication events. The latter include speeches and interviews given by the ECB president, members of the Executive Board of the ECB, and the governors of the national central banks of France, Germany, Italy, and Spain.

To ensure the intermeeting events only capture information about the path of euro area monetary policy, we apply the following filters. First, we retain only those events which generated abnormal returns, as estimated by [Istrefi et al. \(2024\)](#), in at least three of the assets we consider in the high-frequency model. Second, we discard observations which do not fall during market hours or which occur less than one hour after an FOMC policy decision or a macroeconomic data release surprise³. Third, we discard events prior to 2001 to avoid measurement error from the illiquid and underdeveloped OIS market that characterized the early years of the monetary union. The final sample includes 550 events.

The high-frequency model we consider is a Bayesian factor model with regime-dependent

³See [Istrefi et al. \(2024\)](#) for details on the news releases they control for

variances:

$$\mathbf{y}_t = \boldsymbol{\Lambda} \boldsymbol{\epsilon}_t + \mathbf{B} \mathbf{x}_t + \mathbf{v}_t \quad (1)$$

$$\boldsymbol{\epsilon}_t \sim \mathcal{N}(\mathbf{0}, \Sigma_{s_\epsilon}^\epsilon), \quad \mathbf{v}_t \sim \mathcal{N}(\mathbf{0}, \Sigma_{s_v}^v), \quad s_\epsilon, s_v \in \{\text{low, high}\} \quad (2)$$

where \mathbf{y}_t is a $N \times 1$ vector of high-frequency movements in asset prices, $\boldsymbol{\Lambda}$ is a $N \times K$ matrix of factor loadings, $\boldsymbol{\epsilon}_t$ is a $K \times 1$ vector of monetary policy shocks, \mathbf{B} is a $N \times M$ matrix of coefficients, \mathbf{x}_t is a $M \times 1$ vector of financial and economic control variables, and \mathbf{v}_t is a $N \times 1$ vector of idiosyncratic residuals. Both the structural shocks $\boldsymbol{\epsilon}_t$ and the idiosyncratic components \mathbf{v}_t feature regime-switching volatility. This allows us to control for time-varying heteroskedasticity and the empirical regularity that asset price volatility is higher during scheduled GC meetings than intermeeting events.

The model includes 15 variables: OIS yields (1-month, 3-month, 6-month, 1-year, 2-year, 3-year, 5-year, 7-year, and 10-year), Italian sovereign yields (2-year, 5-year, and 10-year), the EURO STOXX 50 stock price index, the Euro/Dollar exchange rate, and the 1-year ILS.

The model also controls for predictability in the high-frequency movements of assets (Bauer and Swanson , 2023) by allowing for a vector of exogenous controls \mathbf{x}_t . Specifically, we include the lagged 3-month changes for the following eight variables: the Composite Indicator of Systemic Stress (Hollo et al., 2012), the monetary policy uncertainty indicator for the euro area (Bauer et al., 2021), the EURO STOXX 50 stock index, Brent crude, the yield curve slope (measured as the difference between the 10-year and 3-month OIS yields), the Germany-Italy 10-year sovereign spread, core HICP inflation, and unemployment.

2.2 Determining the Number of Factors

To determine the dimension K of the structural shocks $\boldsymbol{\epsilon}_t$, and therefore the number of monetary policy instruments, we apply Bayesian LASSO shrinkage with factor-specific hierarchical priors on the factor loadings:

$$\Lambda_{ij} | \lambda_j \sim \text{Laplace}(0, 1/\lambda_j), \quad \lambda_j \sim \text{Gamma}(a_\lambda, b_\lambda) \quad (3)$$

The Bayesian LASSO prior induces adaptive L_1 regularization on the factor loadings

through its hierarchical structure. Each loading Λ_{ij} receives a Laplace prior centered at zero. The Laplace distribution is sharply peaked at zero, and allows for non-zero values only if supported by the data. Factors with weak explanatory power are assigned large λ_j penalty parameters, thereby inducing aggressive shrinkage of the corresponding column of loadings $\mathbf{\Lambda}_{\cdot,j}$ toward zero. The intensity of the shrinkage applied is governed by the hyperparameters (a_λ, b_λ) . During the factor selection phase, we point-identify a rotation of the factors ϵ_t by imposing block-lower triangularity on $\mathbf{\Lambda}$ with positive diagonal elements ([Lopes and West, 2004](#)), and we allow for up to nine factors.

Figure 1 displays the posterior medians of the absolute factor loadings $|\Lambda_{ij}|$. We set $a_\lambda = b_\lambda = 0.25$ for moderate shrinkage⁴. The heatmap reveals four factors with large loadings. The first one primarily affects short-term rates, the second and third load mostly on the middle- and long-end of the yield curve, and the fourth on sovereign yields and stock prices. A fifth factor loads more weakly on longer-dated risk-free and sovereign yields. Based on this evidence, we set $K = 5$.

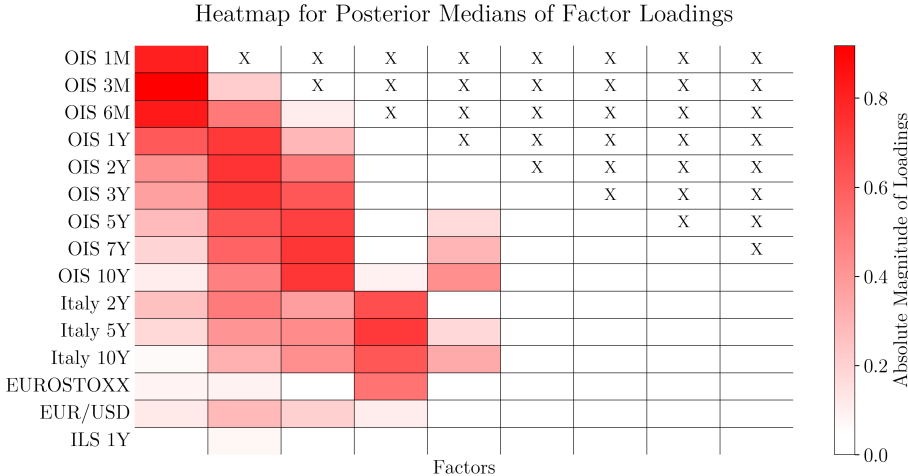


Figure 1: Heatmap for Posterior Medians of Factor Loadings

Note: The heatmap displays the absolute value of posterior median factor loadings $|\Lambda_{ij}|$ under Bayesian LASSO shrinkage. Darker red indicates larger loadings in absolute value. The X symbols denote zero restrictions imposed by the block-lower triangular assumption.

⁴We verify that the results are preserved when varying the values of the hyperparameters (a_λ, b_λ) .

2.3 Identification Strategy

2.3.1 Econometric Framework

Identifying five distinct dimensions of monetary policy in high-frequency data poses substantial challenges. Relying only on zero restrictions (Altavilla et al., 2019; Swanson, 2021) would require ten constraints to achieve point-identification, a demanding requirement. Sign restrictions rely on weaker assumptions but are not sufficient to disentangle multiple monetary policy instruments expected to have qualitatively similar effects on variables. For instance, theory suggests that contractionary shocks operating through conventional policy, forward guidance, or asset purchases all raise yields and the exchange rate while depressing stock valuations and inflation expectations.

We overcome these identification challenges by augmenting sign restrictions with narrative restrictions (Antolín-Díaz and Rubio-Ramírez, 2018) based on well-documented historical episodes. We translate historical evidence into inequality constraints on the posterior of factor loadings by exploiting variations in the relative importance of different shocks across policy events.

For a narrative event at time τ , let shock j be the most important driver of the high-frequency movement of asset i :

$$|\Lambda_{ij}\epsilon_{j\tau}| > \max_{k \neq j} |\Lambda_{ik}\epsilon_{k\tau}| \quad (4)$$

We implement such narrative restrictions on loadings Λ_{ij} using element-by-element Gibbs sampling (Korobilis, 2022). The unrestricted posterior for Λ_{ij} conditional on all other parameters follows from conjugate normal-normal updating:

$$p(\Lambda_{ij} | \cdot) \propto \mathcal{N}(\bar{\mu}_{ij}, \bar{\sigma}_{ij}^2) \quad (5)$$

$$\bar{\sigma}_{ij}^{-2} = \underline{\Omega}_{ij} + \sum_{t=1}^T \frac{\epsilon_{jt}^2}{\sigma_{i,s_v(t)}^v} \quad (6)$$

$$\bar{\mu}_{ij} = \bar{\sigma}_{ij}^2 \left[\underline{\Omega}_{ij}\mu_{ij} + \sum_{t=1}^T \frac{\epsilon_{jt}\tilde{y}_{it}}{\sigma_{i,s_v(t)}^v} - \sum_{k \neq j} \Lambda_{ik} \sum_{t=1}^T \frac{\epsilon_{jt}\epsilon_{kt}}{\sigma_{i,s_v(t)}^v} \right] \quad (7)$$

where the notation $p(\Lambda_{ij}|\cdot)$ denotes the posterior conditional on all other parameters, $\bar{\mu}_{ij}$ and $\bar{\sigma}_{ij}^2$ are the posterior mean and variance of Λ_{ij} , $\underline{\Omega}_{ij}$ and $\underline{\mu}_{ij}$ are the prior precision and mean, $\tilde{y}_{it} = y_{it} - \sum_{m=1}^M B_{im}x_{mt}$ is the residualized asset price movement, and $\sigma_{i,s_v(t)}^v$ denotes the variance of the residual for asset i in regime state $s_v(t)$.

Narrative restrictions truncate the posterior for Λ_{ij} . Let \mathcal{T}_j denote the set of narrative events for shock j . The restricted posterior is given by:

$$p(\Lambda_{ij}|\cdot, \mathcal{A}_{ij}) \propto \mathcal{N}(\bar{\mu}_{ij}, \bar{\sigma}_{ij}^2) \times \prod_{\tau \in \mathcal{T}_j} \mathbf{1}\{\Lambda_{ij} \in \mathcal{A}_{ij}(\tau)\} \quad (8)$$

where $\mathcal{A}_{ij}(\tau)$ is the admissible region defined by the narrative restriction for event τ :

$$\mathcal{A}_{ij}(\tau) = \left\{ \Lambda_{ij} : |\Lambda_{ij}| > \max_{k \neq j} \frac{|\Lambda_{ik}\epsilon_{k\tau}|}{|\epsilon_{j\tau}|} \right\} \quad (9)$$

In practice, we impose sign and narrative restrictions on the loadings Λ_{ij} by sampling from the following truncated normal distribution:

$$\Lambda_{ij} | \cdot \sim \mathcal{TN}(\bar{\mu}_{ij}, \bar{\sigma}_{ij}^2, a_{ij}, b_{ij}) \quad (10)$$

$$\begin{cases} a_{ij} = \max \left\{ 0, \max_{\tau \in \mathcal{T}_j, k \neq j} \frac{|\Lambda_{ik}\epsilon_{k\tau}|}{|\epsilon_{j\tau}|} \right\}, & b_{ij} = \infty \quad \text{if } \Lambda_{ij} > 0 \\ a_{ij} = -\infty, & b_{ij} = \min \left\{ 0, -\max_{\tau \in \mathcal{T}_j, k \neq j} \frac{|\Lambda_{ik}\epsilon_{k\tau}|}{|\epsilon_{j\tau}|} \right\} \quad \text{if } \Lambda_{ij} < 0 \end{cases} \quad (11)$$

where $\mathcal{TN}(\mu, \sigma^2, a, b)$ denotes the Normal distribution with mean μ and variance σ^2 truncated to the interval $[a, b]$. The bounds ensure that shock j is the largest contributor to the movement in asset i for each narrative event $\tau \in \mathcal{T}_j$ while respecting the sign restrictions imposed on Λ_{ij} . This element-by-element⁵ sampling strategy⁶ automatically satisfies both sign and narrative restrictions without having to implement computationally demanding accept/reject algorithms⁷

⁵Element-by-element Gibbs sampling introduces serial correlation in the MCMC draws. To mitigate autocorrelation in posterior samples, we thin the chain by retaining every 5-th draw after the burn-in phase.

⁶Korobilis (2022) implements a similar algorithm in a Bayesian factor model with sign restrictions only.

⁷It should be mentioned, however, that this does not imply one can impose any identifying restriction on the model either. If the restriction is not supported by the data, then the truncated interval $[a, b]$ might be empty or contain negligible posterior probability mass.

2.3.2 Identifying Assumptions

We implement a set of sign and narrative restrictions to set-identify conventional monetary policy (alternatively called target), forward guidance, quantitative easing, asymmetric country risk premia, and information shocks. The first three are the standard policy instruments documented in the literature (Altavilla et al., 2019; Swanson, 2021). The fourth is specific to the euro area currency union and captures diverging sovereign risk premia dynamics between core and peripheral countries (Motto and Özen, 2022; Ricco et al., 2025). Finally, the fifth factor controls for the effects of unexpected shifts in the ECB's assessment of the economic outlook (Nakamura and Steinsson, 2018; Jarociński and Karadi, 2020).

Sign Restrictions. The sign restrictions impose theory-consistent responses following contractionary shocks:

1. Conventional monetary policy, forward guidance, and quantitative easing shocks raise yields and the exchange rate, depress stocks and the ILS.
2. Asymmetric country risk premia shocks raise peripheral yields and lead to declines in risk-free yields (OIS), stocks, and the exchange rate.
3. The information shock induces a positive comovement between all assets (Jarociński and Karadi, 2020).

Narrative restriction for conventional policy (May 10, 2001). Amid a deteriorating economic outlook, the ECB cut interest rates by 25bps to 4.5% for only the second time since its inception in 1998. In doing so, the ECB reversed prior expectations set in earlier public statements that emphasized the central bank's mandate to maintain price stability.

CNN covered the event with an article headlined "ECB surprises with rate cut" and notes "Only three economists out of 50 polled by *Reuters* expected a rate cut." The article reported comments by David Brown, then chief economist at Bear Stearns, who stated "That's got to be the biggest monetary shock of the new millennium [...] They've completely pulled the wool over the market's eyes." Similarly, *Forbes* reported "A very surprising European Central Bank interest rate cut propelled stock markets in Europe higher [...] The move [...] came as a surprise to most observers [...]" This restriction is imposed on the 1-, 3-, and

6-month OIS yields, the stock price index, the Euro/Dollar exchange rate, and the 1-year ILS.

Narrative restriction for forward guidance (December 15, 2022). During the post-pandemic inflation surge, the ECB issued hawkish forward guidance stating that "based on the substantial upward revision to the inflation outlook, expects to raise them [interest rates] further. In particular, the Governing Council judges that interest rates will still have to rise significantly at a steady pace". The press release reiterates again, in a new passage compared to the previous press release, that "The Governing Council decided to raise interest rates today, and expects to raise them significantly further" and changed "Inflation [...] will stay above the target for an extended period" to "inflation [...] is projected to stay above the target for too long." It also adds the following new passage "underlying price pressures across the economy have strengthened and will persist for some time".

The next day, the *Financial Times* covered the event with the headline "Lagarde admits ECB 'in for the long game' on rate rises". Similarly, the *New York Times* reports "Europe's Central Banks Raise Rates, and Prepare for More". This restriction is imposed on the 1-, 2-, and 3-year OIS yields, the stock price index, the Euro/Dollar exchange rate, and the 1-year ILS.

Narrative restriction for quantitative easing (January 22, 2015). Mario Draghi confirmed circulating rumours of further monetary stimulus beyond an interest rate cut with the announcement of the asset purchase programme (APP) starting in March 2015 and with monthly purchases of €60 billion per month. The decision was partially leaked the previous evening and therefore anticipated by markets, but the scale of purchases exceeded expectations.

The main headline on the *Financial Times* Europe edition cover page on January 23, 2015 reads "Markets rally as ECB bond-buying plan exceeds investor expectations." Similarly, the *New York Times* writes "Mario Draghi, said [...] would begin buying bonds worth 60 billion euros, [...] a month. That is more spending than the €50 billion a month that many analysts had been expecting." One of the largest quantitative easing shocks identified by [Altavilla et al. \(2019\)](#). This restriction is imposed on the 5-, 7-, and 10-year OIS yields, the 5- and 10-year Italian sovereign yields, the stock price index, the Euro/Dollar exchange rate, and

the 1-year ILS.

Narrative restriction for asymmetric country risk (July 26, 2012). This event corresponds to the "whatever it takes" speech given by Mario Draghi in London and during which he pledged an unlimited commitment towards the Euro, stating "Within our mandate, the E.C.B. is ready to do whatever it takes to preserve the euro. And believe me, it will be enough [...] the euro is irreversible."

The *New York Times* reported on the speech with an article titled "Assurances on Euro by Central Bank Chief Lift Stocks". Similarly, *CNN* titles an article "Draghi to the rescue". This restriction is imposed on the 2-, 5-, and 10-year Italian sovereign yields, the stock price index, the Euro/Dollar exchange rate, and the 1-year ILS.

3 Euro Area Monetary Policy Shocks

In this section, we present the identified high-frequency monetary policy shocks for the euro area. We tie these to the narrative record and discuss the relevance of information shocks. We then relate our identified shock series with the literature.

3.1 Identified Shocks

Although the restrictions we impose are set-identifying only, the monetary policy factors we recover are tightly identified. Figure 2 displays the columns of the loadings matrix Λ along with 95% highest posterior density (HPD) bands together with the time series for the identified shocks. Figure 3 presents the same plots for information shocks.

Conventional monetary policy predominantly affects short-term interest rates, with impacts declining smoothly along the yield curve. Forward guidance operates through the middle and long end of the yield curve while leaving short-term rates largely unchanged, and generates substantial exchange rate movements. Quantitative easing shocks only affect yields with maturities exceeding five years. Asymmetric country risk premia shocks trigger flight-to-safety dynamics: they moderately depress long-dated risk-free yields while sharply elevating peripheral sovereign yields, and they simultaneously generate strong reactions in both equity markets and the exchange rate. Finally, the information shock closely resembles

forward guidance in its term structure effects but induces positive comovements between yields and stock prices.

The identified shocks align closely with the historical record. The largest expansionary conventional shock identified captures the coordinated response to the 9/11 attacks, when on September 17, 2001 the ECB cut rates by 50 basis points along with the Federal Reserve and other major central banks. The largest contractionary forward guidance shock occurred on June 5, 2008, when amid rising inflationary pressures the ECB held rates at 4% while Trichet issued hawkish guidance. The *New York Times* noted the ECB "warned unexpectedly that it might raise interest rates next month," though markets had expected rates to remain steady. Lehman Brothers would collapse just two months later.

The largest contractionary quantitative easing shock happened on December 3, 2015, when the ECB maintained the prevailing monthly rate of asset purchases under the APP, disappointing market expectations of further expansion. The *Financial Times* headlined "Market sell-off as fresh Draghi bid to boost growth disappoints". Finally, the largest contractionary asymmetric country risk premia shock occurred on March 12, 2020 when ECB President Christine Lagarde stated the bank was "not here to close spreads," triggering a widening in peripheral sovereign spreads⁸.

The time series plots also reflect the evolving nature of euro area monetary policy. Prior to the financial crisis, policy was conducted exclusively through conventional interest rate adjustments and forward guidance. During the European sovereign debt crisis, asymmetric country risk premia shocks became the most important drivers of high-frequency movements in asset prices around policy events. As the ECB reached the zero lower bound, asset purchases became the primary policy instrument in the mid-2010s. Finally, all policy tools were simultaneously used during the post-pandemic inflation surge; see Appendix Figure 1.

⁸In a *CNBC* interview later that day, she reversed course, stating "I am fully committed to avoid any fragmentation in a difficult moment for the euro area"

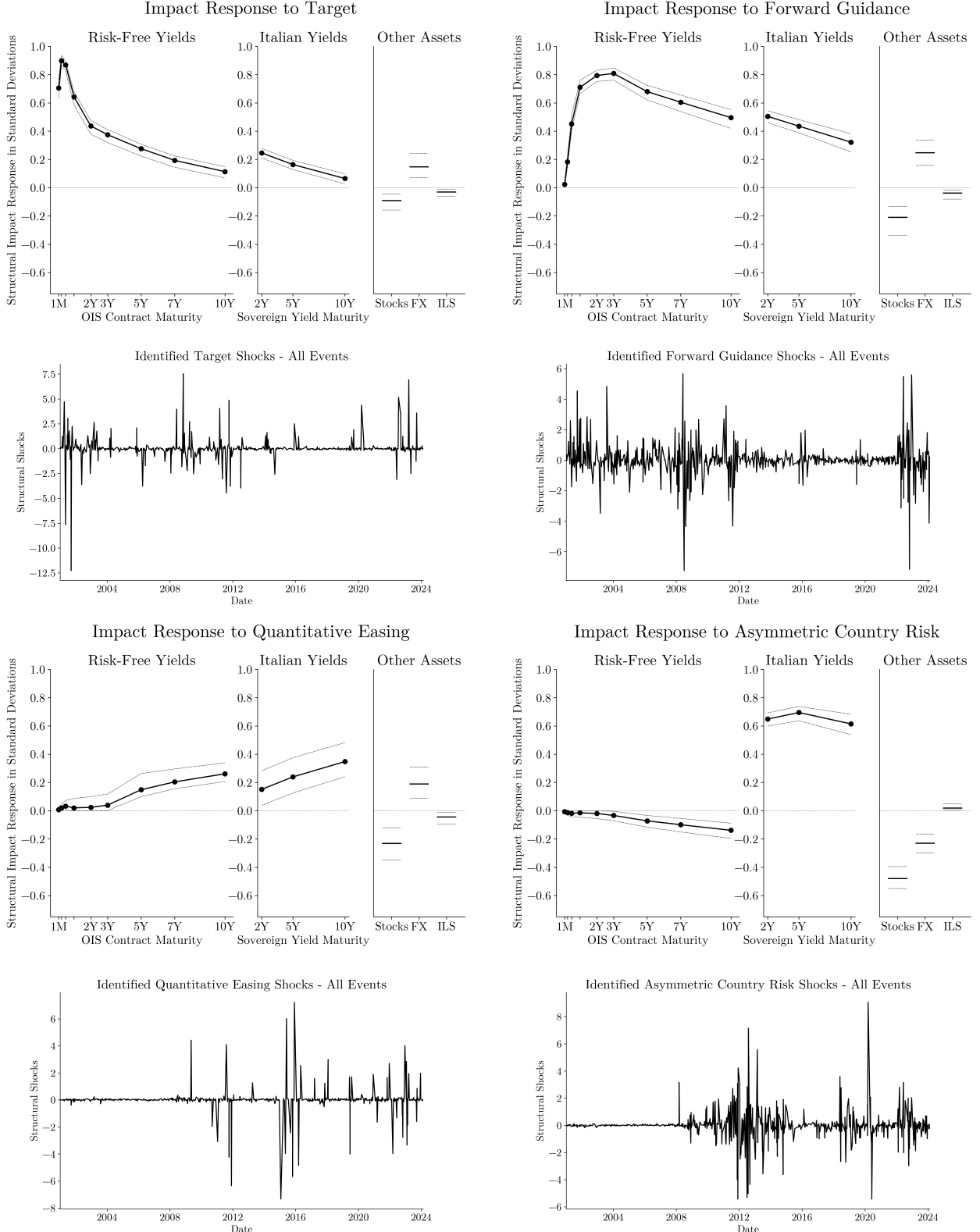


Figure 2: Identified Monetary Policy Shocks: Impact Matrix Λ and Time Series

Notes: The first and third rows display posterior medians of factor loadings $\Lambda_{\cdot,j}$ along with 95% HPD bands for each shock, with the shocks normalized to have unit variance. The second and fourth rows show the identified shock time series ϵ_{jt} over the sample period.

3.2 The Role of Information Shocks

The time series plots reveal substantial time-varying heteroskedasticity and heavy tails⁹ in the monetary policy shocks. The information shock, however, exhibits markedly different behavior. Unlike the four policy shocks, the information shock series appears extremely noisy and fails to map onto identifiable historical episodes. The largest contractionary information shock identified corresponds to a speech on payment systems which did not reveal any material information about the economic outlook¹⁰. Most large information shocks are identified during intermeeting events, in contrast to the monetary policy shocks for which large realizations occur predominantly during GC meetings.

Figure 4 reveals substantial tail deviations from normality for all policy shocks, while information shocks are concentrated around the mean and close to being Normal. Across posterior draws, the ratio of high-state to low-state variance ranges from 30 to 350 for monetary policy shocks, but stands at just 2.7 for information shocks.

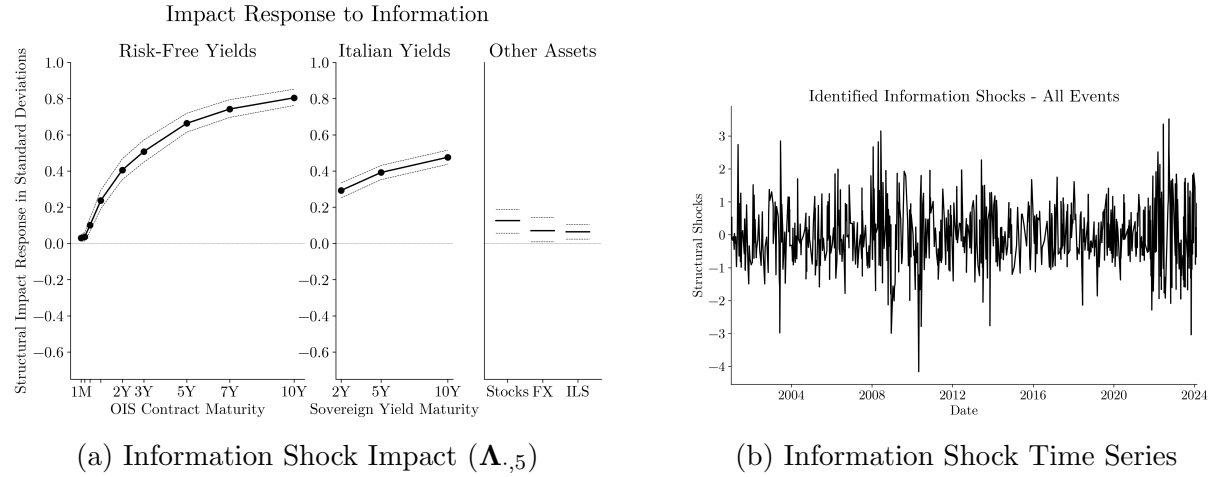


Figure 3: Information Shock: Structural Impact and Time Series

Note: Panel (a) displays posterior medians of factor loadings $\Lambda_{.,5}$ along with 95% HPD bands for the information shock, with the shock normalized to have unit variance. Panel (b) shows the identified shock time series ϵ_{5t} over the sample period.

Furthermore, Table 1 shows that monetary policy uncertainty (Bauer et al., 2021) and the composite indicator of systemic risk (CISS) (Hóollo et al., 2012) are significant predictors

⁹We estimate negligible cross-correlations among squared monetary policy shocks. This finding, together with the high kurtosis of the identified shocks, provides support for identification strategies that exploit non-Gaussianity and shock independence (Jarociński, 2024).

¹⁰The transcript for the speech can be accessed [here](#).

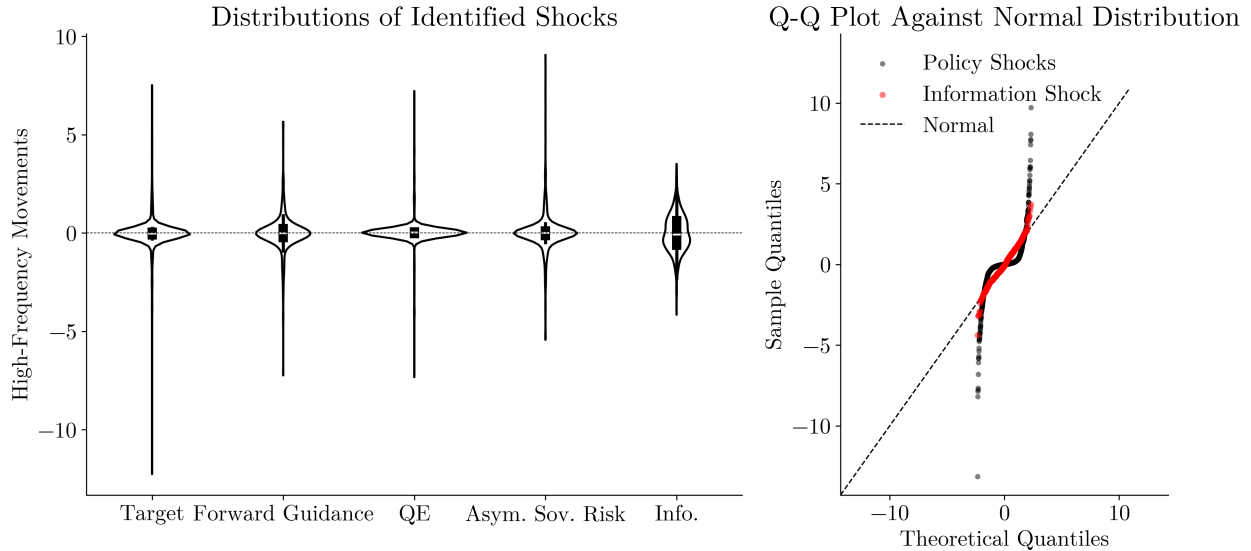


Figure 4: Distributions of Identified Structural Shocks

Note: The left panel shows violin plots of the identified structural shocks. The right panel displays Q-Q plots against the normal distribution, with policy shocks (conventional policy/target, forward guidance, quantitative easing, and asymmetric country risk premia) pooled together in black and the information shock shown separately in red. Deviations from the 45-degree line indicate departures from normality.

of high-frequency movements in several risk-free and sovereign yields at maturities of two years and greater, segments of the yield curve generally associated with information effects. This confirms findings by [Bauer and Swanson \(2023\)](#) and [Ricco et al. \(2025\)](#) that high-frequency surprises are partially predictable. The estimates in Table 1 imply that, when systemic stress is high, the ECB provides less accommodation than expected by markets, and vice versa when there is uncertainty regarding the stance of monetary policy.

These observations suggest that the identified information shocks may in fact capture residual positive comovements across assets—fluctuations that, by construction, cannot be attributed to the other four shocks given the sign restrictions we impose.

3.3 Comparison with the Literature

We also verify that the shocks we identify correlate with those previously identified in the literature. In Table 2, we compute the Pearson and rank correlations between our identified shocks and the ones derived by [Altavilla et al. \(2019\)](#). They consider seven OIS yields in their

Table 1: Predictability of High-Frequency Movements in Financial Assets

	CISS	MP Uncer.	STOXX50	Oil Price	Yield Slope	DE-IT Spread	Core HICP	Unemp.
OIS 1M	0.01	-0.01	-0.02*	-0.01	0.00	-0.02	0.00	0.00
OIS 3M	-0.02	-0.01	-0.03*	-0.01	0.01	0.01	0.01	0.01
OIS 6M	0.02	-0.03	-0.01	-0.03	0.03	0.01	0.01	0.01
OIS 1Y	0.04	-0.05*	0.01	-0.02	0.02	0.02	0.00	0.00
OIS 2Y	0.11***	-0.08***	0.03	-0.04	0.02	0.02	-0.03	0.02
OIS 3Y	0.12***	-0.09***	-0.01	-0.06	0.03	0.02	-0.03	0.02
OIS 5Y	0.10**	-0.07**	0.00	-0.08	0.03	0.01	-0.04	0.02
OIS 7Y	0.11**	-0.06*	-0.01	-0.11	0.02	0.02	-0.05	0.02
OIS 10Y	0.11**	-0.05	-0.02	-0.11	0.02	0.02	-0.05	0.03
IT 2Y	0.07**	-0.06***	-0.02	-0.03	0.02	0.01	-0.04	0.01
IT 5Y	0.06**	-0.06***	-0.01	-0.00	0.02	0.00	-0.05	0.01
IT 10Y	0.08**	-0.05**	-0.02	-0.01	0.02	-0.01	-0.02	0.02
EUROSTOXX	-0.01	0.01	-0.00	-0.04	0.07	0.01	-0.04	-0.05*
EUR/USD	0.05	-0.03	-0.01	-0.01	0.04	0.01	-0.05	0.01
ILS 1Y	-0.00	0.07**	0.02	-0.01	0.08	-0.02	0.01	0.01

Notes: This table reports coefficient values \mathbf{B} associated with the control variables \mathbf{x}_t . *, **, and *** denote that zero is not contained in the 90%, 95%, and 99% HPD intervals, respectively.

specification. Our target and forward guidance shocks correlate strongly with theirs, though they also correlate with the additional near-term forward guidance shocks (Timing) they identify. On the other hand, their quantitative easing shocks are positively correlated with our residual information shocks. This may reflect the fact that they do not impose restrictions inducing negative comovements between yields and stock prices, such that their quantitative easing shocks may incorrectly capture positive comovements between these assets.

The shocks we identify also align with the narrative restrictions used by [Badinger and Schiman \(2023\)](#). One of the events they use in their narrative analysis is the GC meeting on November 6, 2008, when the ECB cut rates by 50 basis points, disappointing markets after the Bank of England had slashed its policy rate by 150 basis points less than two hours earlier. We identify this as the largest contractionary target shock. They also use the October 6, 2011, GC meeting when Trichet held rates constant but emphasized inflation risks on the upside, while most market participants had either expected rates to remain unchanged or cut. We identify this episode as the fourth largest contractionary shock in our sample. This was followed by the surprise 25 basis point rate cut by Mario Draghi on November 3, 2011. The cut, which occurred during Draghi’s first GC meeting, was perceived as a shift toward a more dovish policy stance and reversed expectations that Trichet had set

in motion at his final GC meeting. This is the fifth largest expansionary target shock we identify.

Table 2: Correlation of Identified Shocks with [Altavilla et al. \(2019\)](#)

ABGMR 2019	Target	Forward Guidance	Quantitative Easing	Asymmetric Country Risk	Information
Target	0.73 (0.59)	-0.15 (-0.03)	0.10 (0.15)	0.05 (-0.04)	0.09 (0.17)
Timing	0.52 (0.58)	0.29 (0.21)	0.23 (0.26)	-0.12 (-0.13)	-0.07 (-0.06)
Forward Guidance	0.23 (0.16)	0.72 (0.71)	0.15 (0.02)	-0.01 (-0.10)	0.22 (0.24)
Quantitative Easing	-0.04 (-0.08)	0.04 (0.01)	0.48 (0.36)	-0.29 (-0.19)	0.63 (0.69)

Notes: This table reports Pearson correlation coefficients between shocks identified in this paper and those from [Altavilla et al. \(2019\)](#) over the common sample of ECB GC meetings. Spearman rank correlations are shown in parentheses.

4 The Macroeconomic Effects of Monetary Policy

In this section, we present the macroeconometric model used to trace out the impact of monetary policy shocks on economic outcomes. We then present our estimates and discuss their sensitivity to the identifying assumptions we impose.

4.1 Econometric Methodology

We study the aggregate dynamic causal effects of monetary policy instruments using a Bayesian VAR-DL with time-varying volatility:

$$\mathbf{y}_t = \sum_{l=1}^p \Phi_l \mathbf{y}_{t-l} + \sum_{j=0}^q \Psi_j m_{t-j} + \mathbf{v}_t \quad (12)$$

$$\mathbf{v}_t \sim \mathcal{N}(\mathbf{0}, \Sigma_t) \quad (13)$$

$$\Sigma_t = e^{h_t} \Sigma \quad (14)$$

$$h_t = \rho_h h_{t-1} + u_t^h, \quad u_t^h \sim \mathcal{N}(0, \sigma_h^2) \quad (15)$$

where \mathbf{y}_t is an $n \times 1$ vector of endogenous variables, Φ_l are $n \times n$ autoregressive coefficient matrices, p is the number of autoregressive lags, m_t denotes the aggregated high-frequency monetary policy shocks, Ψ_j are $n \times 1$ distributed lag coefficient vectors, and q is the number of distributed lags for the shock. Following [Carriero et al. \(2016\)](#), we model time-varying volatility with a single common factor that proportionally scales all covariances. This parsimonious specification controls for heteroskedasticity, which is particularly important when including the pandemic era in the sample, see Appendix Figure 2.

The Bayesian VAR-DL framework offers several advantages in our setting. First, as shown by [Baek and Lee \(2022\)](#), impulse-response coefficients are asymptotically unbiased up to horizon $H \leq q$. In fact, autoregressive distributed lags models are equivalent to local projections with additional controls for the future realizations of the shocks, thus improving efficiency ([Montiel Olea et al., 2025](#)). Second, the Bayesian implementation allows us to propagate the uncertainty surrounding the high-frequency estimates of the monetary policy shocks by directly sampling m_t at each MCMC iteration from the posterior draws obtained from the Bayesian factor model¹¹. As such, Bayesian methods allow us to overcome a major difficulty when using distributed lag models in frequentist settings where the shock series m_t either needs to be observed or estimates need to be adjusted for generated regressors.

In addition, this framework allows us to impose overidentifying zero, sign, or magnitude restrictions on the impulse-responses to sharpen identification¹². Moreover, Bayesian shrinkage can be applied to the autoregressive matrices Φ_l to facilitate the choice of lags p . Finally, it is also possible to trade off higher bias for lower variance in the impulse-response estimates by either (i) penalizing the differences in consecutive impulse-responses coefficients to impose smoothness or (ii) shrinking impulse-responses toward low-order polynomials. In our application, we find that the former leads to considerably smoother responses at the cost of minimal bias. Specifically, for each equation i , let $\psi_i = [\psi_{i,0}, \psi_{i,1}, \dots, \psi_{i,q}]'$ denote the $(q+1) \times 1$ vector of distributed lag coefficients on the monetary policy shock, where $\psi_{i,j}$ is the i -th element of Ψ_j . We impose a Bayesian ridge prior that penalizes d -th order

¹¹In contrast, most studies treat identified high-frequency monetary policy shocks as data. A notable exception is [Jarociński and Karadi \(2025\)](#) who employ a similar strategy to ours.

¹²For impact restrictions, one can directly truncate the posterior for ψ_j . For restrictions at longer horizons, one can use an accept/reject procedure instead.

differences:

$$\boldsymbol{\psi}_i | \cdot \sim \mathcal{N} \left(\mathbf{0}, (\mathbf{I}_{q+1} + \lambda_i^d \mathbf{P})^{-1} \right) \quad (16)$$

where $\mathbf{P} = \mathbf{D}'\mathbf{D}$ is the $(q+1) \times (q+1)$ penalty matrix, \mathbf{D} is the $(q+1-d) \times (q+1)$ d -th order difference operator, and $\lambda_i^d > 0$ controls the degree of smoothing for equation i . For second-order differences ($d=2$), the prior penalizes large changes in the slope of the impulse-response function, and the $(q-1) \times (q+1)$ difference matrix is given by:

$$\mathbf{D} = \begin{bmatrix} 1 & -2 & 1 & 0 & \cdots & 0 \\ 0 & 1 & -2 & 1 & \cdots & 0 \\ \vdots & \ddots & \ddots & \ddots & \ddots & \vdots \\ 0 & \cdots & 0 & 1 & -2 & 1 \end{bmatrix} \quad (17)$$

The penalty parameter λ_i^d is estimated from the data using a hierarchical prior $\lambda_i^d \sim \text{Gamma}(\alpha_{\lambda^d}, \beta_{\lambda^d})$, where we set a proper but very diffuse prior $\alpha_{\lambda^d} = \beta_{\lambda^d} = 0.001$. The conditional posterior for λ_i^d is:

$$\log(p(\lambda_i^d | \cdot)) = (\alpha_{\lambda^d} - 1) \log(\lambda_i^d) - \beta_{\lambda^d} \lambda_i^d + \frac{1}{2} \log(\det(\mathbf{I}_{q+1} + \lambda_i^d \mathbf{P})) - \frac{1}{2} (\boldsymbol{\psi}_i' \boldsymbol{\psi}_i + \lambda_i^d \boldsymbol{\psi}_i' \mathbf{P} \boldsymbol{\psi}_i) \quad (18)$$

which we sample using a random-walk Metropolis-Hastings step on the logarithmic scale to ensure positivity. We discuss polynomial shrinkage and the other posterior distributions in Appendix A.2.

4.2 Model Specification

The specification we consider includes six variables at monthly frequency: the main policy rate, which is either the OIS 3-month yield for target shocks, the OIS 2-year yield for forward guidance shocks, the 10-year German sovereign yield for quantitative easing shocks, or the 2-year Italian sovereign yield for asymmetric country risk premia shocks; industrial production, HICP inflation, real GDP¹³, the real effective exchange rate based on a trade-weighted basket of 42 currencies, and M2 money supply. All the time series were downloaded from the ECB

¹³We linearly interpolate monthly real GDP.

data portal. All variables enter in logarithms except for the policy rate, which enters in levels, and HICP inflation, which is computed as the logarithmic difference of the HICP index.

Given prior evidence that the effects of monetary policy take 12 to 18 months to fully materialize, we conservatively set $q = 24$ and consider a similar forecast horizon. We set $p = 3$ and impose standard Minnesota priors¹⁴ on the matrices Φ_l . The sample covers 2001M1-2024M2, and for quantitative easing and asymmetric country risk premia shocks we start the analysis in January 2008 instead.

Identifying the effects of unconventional monetary policy instruments is challenging without additional restrictions given the small sample sizes and the relatively sparse set of large monetary policy shocks identified (see Figure 2). Therefore, we impose the following overidentifying sign restrictions for two quarters following impact: contractionary monetary policy must raise the relevant policy rate and the real exchange rate while depressing industrial production, GDP, inflation, and money supply. For asymmetric country risk premia shocks, we do not restrict the response of inflation since it is ex-ante unclear whether prices will fall due to lower economic activity or rise as a result of declining exchange rates. All of the sign restrictions imposed are consistent with the impact high-frequency responses shown in Figure 2 and standard predictions from theoretical models. Finally, we impose second-order difference shrinkage ($d = 2$) on the impulse-response coefficients following Equations (16)-(17). We discuss the implications of the sign restrictions and shrinkage on the estimates below.

4.3 Results

All the figures we present depict the impulse-responses to a monetary policy shock rescaled to produce a 25 basis points peak response in the corresponding policy rate. We report the posterior medians of the impulse-responses along with 16th and 84th percentile HPD bands.

Overall, conventional monetary policy shocks induce the largest responses. The response in the OIS 3-month yield is very persistent and remains stable for nine months before revert-

¹⁴We set the overall tightness parameter to 0.2, the cross-lag shrinkage multiplier to 0.5, and the lag decay exponent to 1.

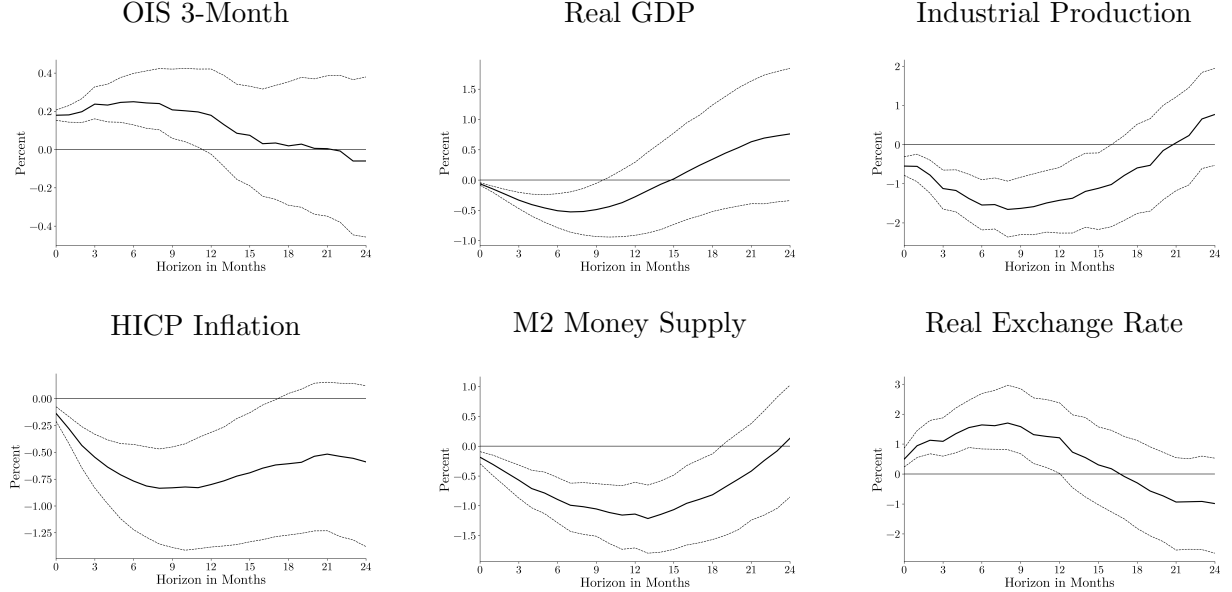
ing to trend, confirming the shocks we identify in the high-frequency sample also capture movements in interest rates at lower frequencies. A 25 basis points peak increase in the 3-month OIS yield leads to a decline in real GDP of up to 0.5% between six to nine months following the shock. Industrial production reacts more strongly, with a trough exceeding 1.5% after nine months. HICP inflation reacts immediately and its response attains a maximum decline of 0.75% after nine months and remains below trend over the entire forecast horizon.

Responses to forward guidance shocks are generally much more muted and effects take longer to materialize, despite movements in the OIS 2-year yield being comparable to the response of the 3-month OIS yield to target shocks. Real GDP falls by only 0.25% in the first year following the shock, with the response slowly declining to -0.5% after two years, but uncertainty bands are wide at longer horizons. Industrial production exhibits similar patterns. HICP inflation falls at most by 0.1% over the forecast horizon, and both money supply and the real exchange rate react less strongly than for conventional policy shocks.

Quantitative easing shocks induce larger responses than forward guidance shocks. The responses for inflation, industrial production, and money supply are qualitatively similar to but slightly smaller than for target shocks. In contrast, the real exchange rate rises very persistently, jumping by 1% on impact and reaching a peak response above 3% after six months before slowly reverting to trend.

Finally, asymmetric country risk premia shocks induce a very persistent response in the sovereign Italian 2-year yield. Nonetheless, the responses of all other economic variables are generally muted and smaller in magnitude than for the other shocks. GDP and industrial production fall moderately over the forecast horizon, reaching troughs close to 0.5% after two years. On the other hand, inflation rises moderately by 0.1%, but there is considerable uncertainty surrounding the estimates (recall we do not impose sign restrictions for this response). Therefore, the inflationary impact of currency depreciation dominates the disinflationary effects resulting from weakening economic activity, thus giving rise to stagflationary dynamics.

Responses to Conventional Monetary Policy Shocks



Responses to Forward Guidance Shocks

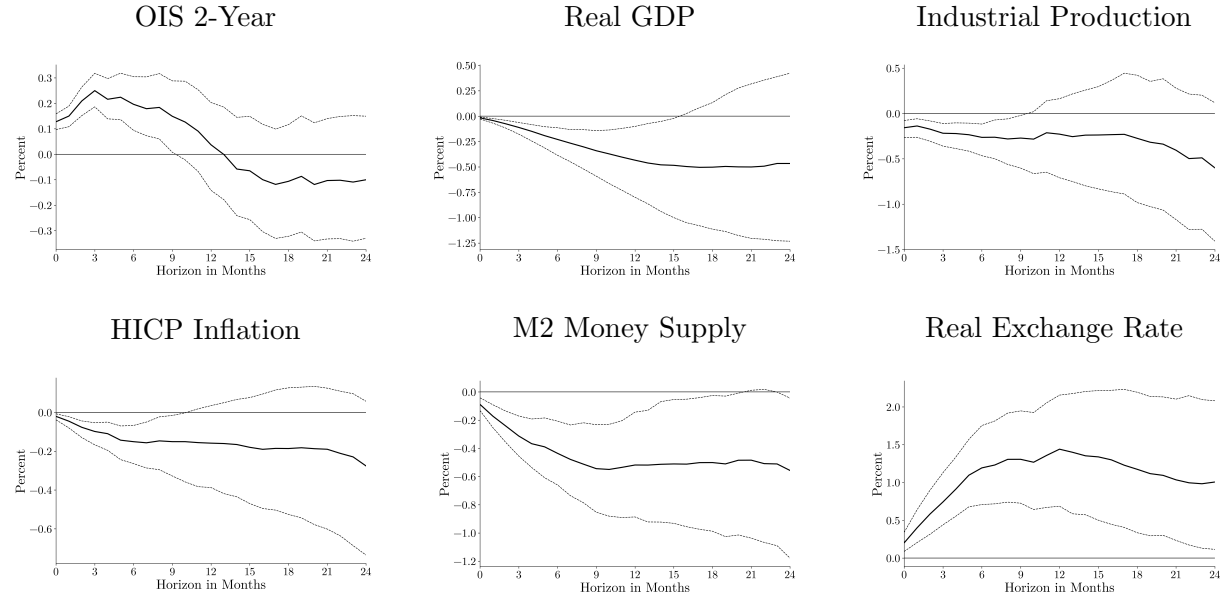
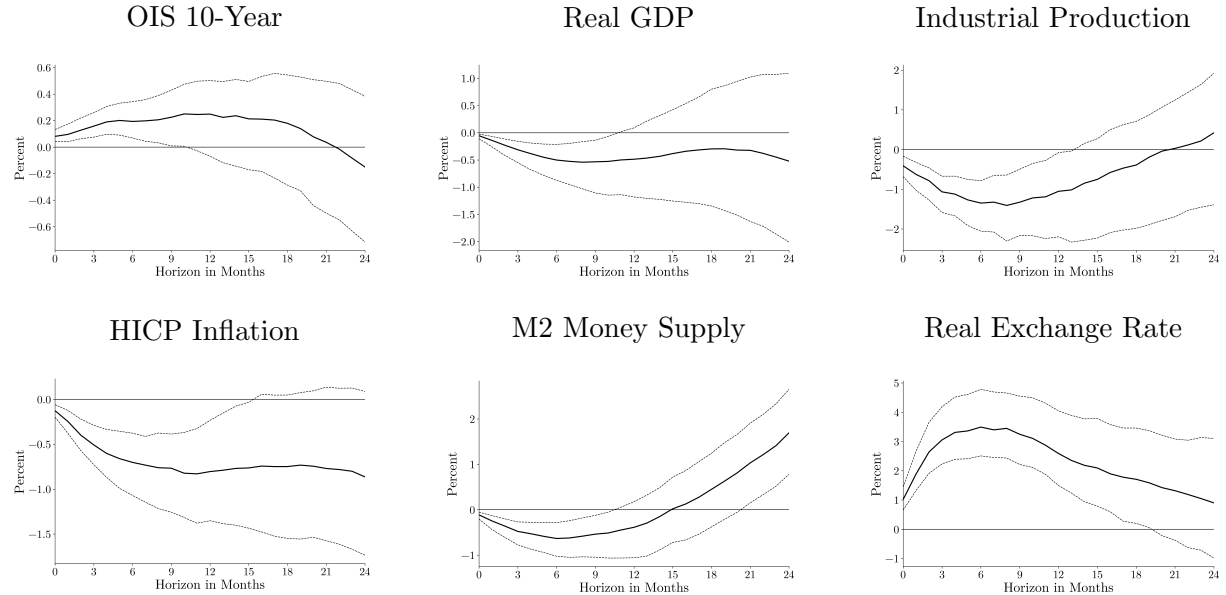


Figure 5: Impulse-Responses to Target and Forward Guidance Shocks

Note: Impulse-responses to contractionary monetary policy shocks. Responses to target shocks rescaled to induce a peak response of 25bps in the OIS 3-month yield. Responses to forward guidance shocks rescaled to induce a peak response of 25bps in the OIS 2-year yield. The solid black line shows the posterior median response, while the bands correspond to the 16th and 84th percentile HPD bands. See text for a description of the model and identifying assumptions.

Responses to Quantitative Easing Shocks



Responses to Asymmetric Risk Country Premia Shocks

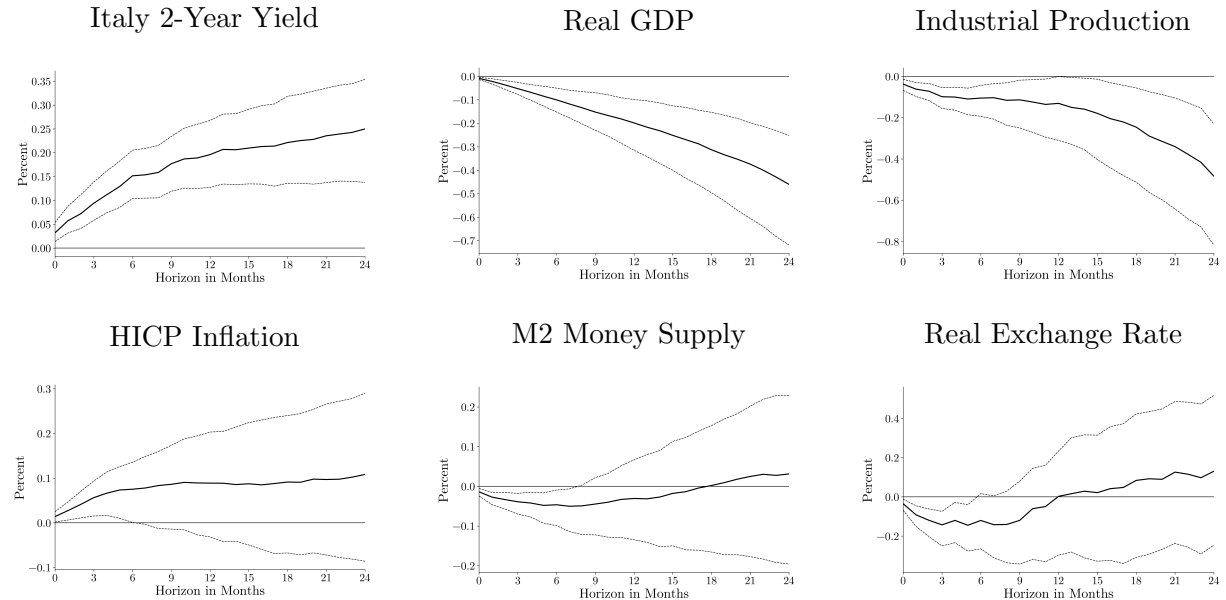


Figure 6: Impulse-Responses to Quantitative Easing and Asym. Risk Country Premia Shocks

Note: Impulse-responses to quantitative easing and asymmetric risk country premia shocks. Responses to quantitative easing shocks rescaled to induce a peak response of 25bps in the OIS 10-year yield. Responses to asymmetric risk country premia shocks rescaled to induce a peak response of 25bps in the Italian 2-year government bond yield. The solid black line shows the posterior median response, while the bands correspond to the 16th and 84th percentile HPD bands. See text for a description of the model and identifying assumptions.

4.4 Alternative Specifications

In Figure 7, we assess the sensitivity of the impulse-response estimates to the overidentifying sign restrictions we impose. We plot responses for the yield associated with each shock, industrial production, and HICP inflation for sign restrictions either imposed for 2 quarters (baseline), 1 quarter, or on impact only.

The responses remain broadly similar across specifications with two exceptions. First, the magnitude of the responses is larger when imposing dynamic sign restrictions. In particular, dynamic sign restrictions sharpen the identification of the 10-year German sovereign yield response to quantitative easing shocks, thus pointing to possible weak identification concerns when relying solely on the high-frequency proxy. Such issues are largely unavoidable given the limited 16-year sample available for this instrument.

Second, the response for industrial production (and to a lesser extent inflation) to forward guidance shocks displays puzzling behaviors without dynamic sign restrictions. Other studies relying on high-frequency instruments have also documented similar puzzles in the responses to forward guidance shocks, see for instance [Miranda-Agricoppino and Ricco \(2023\)](#), [Swanson \(2024\)](#), and [Ricco et al. \(2025\)](#). Note that such puzzles occur despite the fact that we control for predictability in the high-frequency asset movements and allow for residual information shocks.

Overidentifying dynamic sign restrictions are able to rule out these pathological behaviors and induce responses in industrial production and HICP inflation that remain negative over the entire forecast horizon. Again, it is important to underline that were the sign restrictions rejected by the data, then one would be unable to sample from the truncated posterior for the distributed lag coefficients Ψ_j . Nevertheless, these findings suggest that additional research is needed to understand the extent to which high-frequency asset movements around policy events capture endogenous responses by central banks to past macroeconomic shocks, and how to effectively control for these confounding factors.

In Figure 8, we assess the sensitivity of our estimates to the shrinkage priors we impose on the impulse-response coefficients. The difference shrinkage prior is very effective at smoothing the impulse-responses, which otherwise exhibit the jaggedness characteristic of distributed

lag and local projection estimators. At the same time, posterior medians remain broadly unchanged across both specifications, and none of the substantive conclusions we reach are materially affected by shrinking the impulse-response coefficients¹⁵.

5 Conclusion

In this paper, we develop a novel identification strategy that combines narrative restrictions with high-frequency data to separately identify multiple dimensions of euro area monetary policy. Drawing on pivotal ECB policy episodes, we impose a single narrative restriction per shock and are able to disentangle conventional policy, forward guidance, quantitative easing, and asymmetric country risk premia shocks. This approach avoids the challenging requirement that, ex-ante, many assets do not respond to some policy shocks.

Our high-frequency Bayesian factor model, which accounts for both predictability in asset price movements and time-varying volatility, reveals that information shocks exhibit markedly different behavior from policy shocks: they are noisy, fail to align with identifiable historical episodes, and display negligible time-varying heteroskedasticity. These findings suggest that the positive comovements typically attributed to information effects may instead reflect residual variation in asset prices unaccounted for by other shocks.

The macroeconomic analysis reveals substantial heterogeneity in the transmission of monetary policy across instruments. Conventional policy shocks generate the largest responses, whereas forward guidance transmits with longer lags and produces considerably weaker effects. The magnitude of quantitative easing effects lies between those of forward guidance and conventional policy.

These findings carry important implications for monetary policy design in the euro area. The limited effectiveness of forward guidance suggests that managing expectations about the future path of short-term rates provides only modest stimulus compared to actual changes in current rates or asset purchases. Asymmetric country risk premia shocks present a distinct challenge for euro area policymakers as they produce stagflationary dynamics wherein

¹⁵However, it remains important to compare a specification that sacrifices some bias for variance reduction with one that only prioritizes low bias, as we do here following the recommendations of Montiel Olea et al. (2025).

Responses to Conventional Monetary Policy Shocks

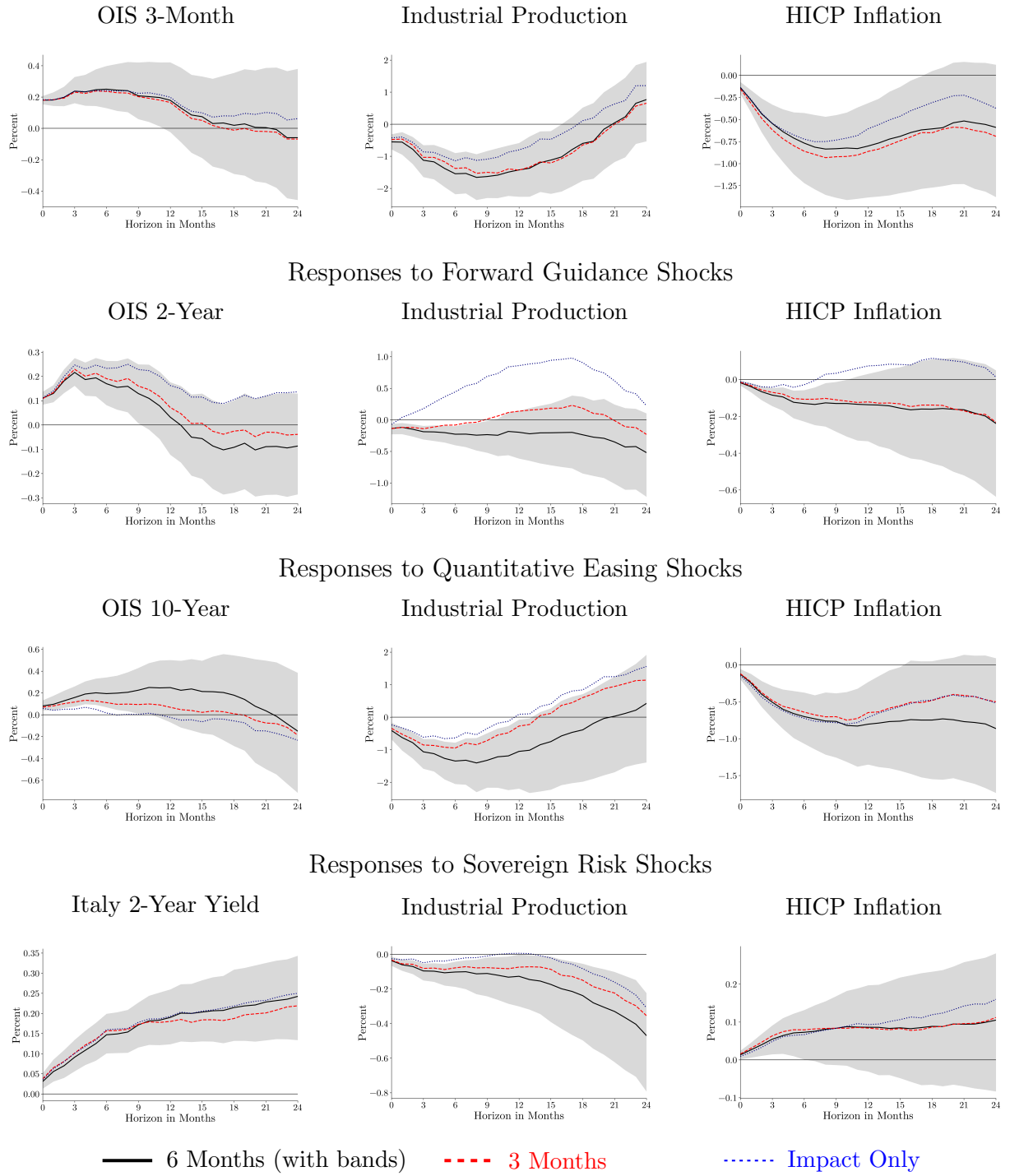


Figure 7: Sensitivity to Sign Restriction Duration

Note: Impulse-responses to all monetary policy shocks under different sign restriction durations. All shocks induce a peak response of 25bps in their respective yields. The solid black line shows the posterior median response with shaded 68% HPD bands for the baseline 2-quarter restriction specification. Dashed red and dotted blue lines show median responses for 1-quarter and impact-only restrictions, respectively. See text for a description of the model and identifying assumptions.

Responses to Conventional Monetary Policy Shocks

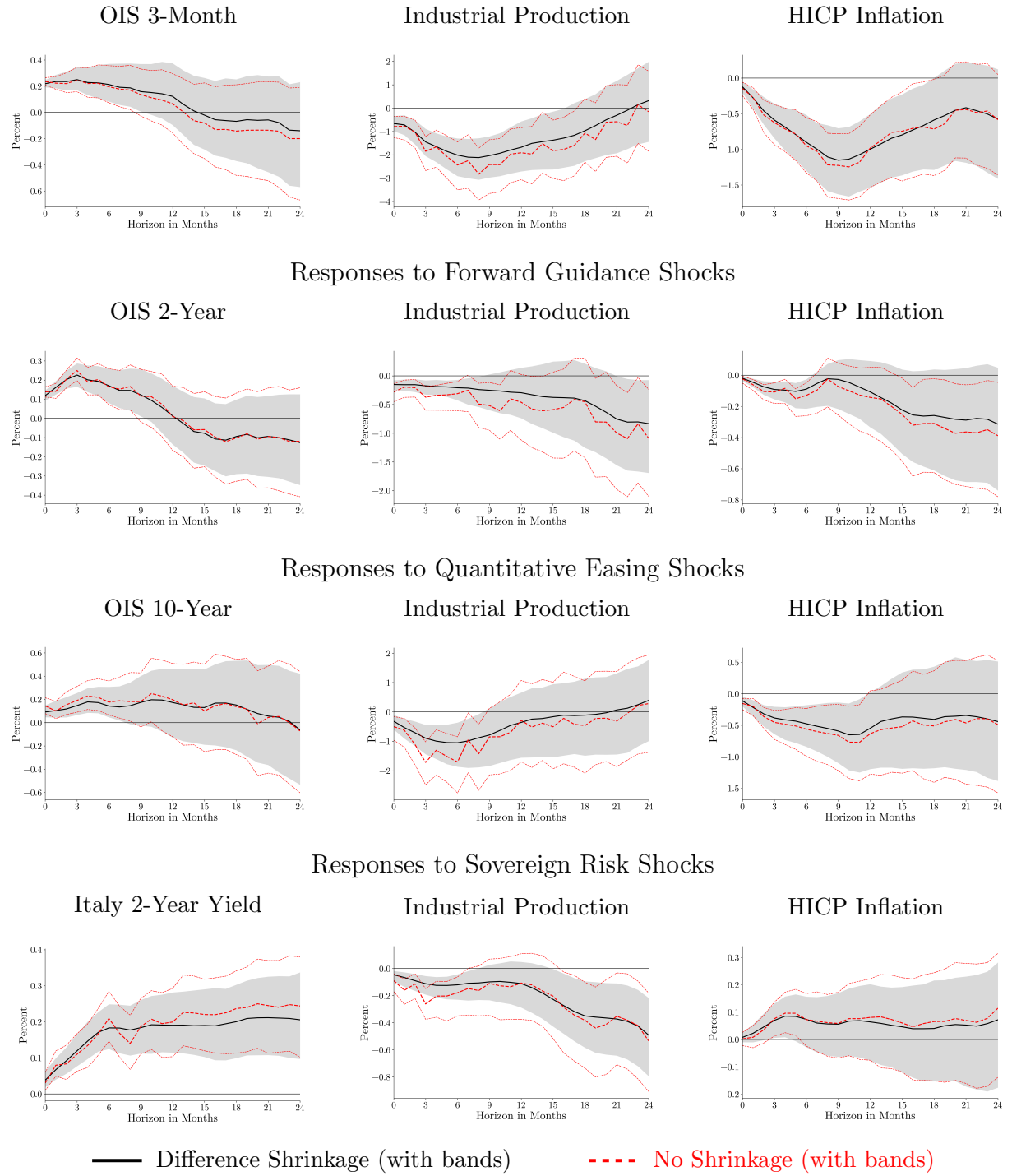


Figure 8: Sensitivity to Smoothing Prior Specification

Note: Impulse-responses to all monetary policy shocks with and without difference shrinkage priors on the distributed lag coefficients. All shocks induce a peak response of 25bps in their respective yields. Solid black lines with shaded bands and dashed red lines with dashed bands show posterior median responses and 68% HPD bands for specifications with and without shrinkage, respectively. See text for a description of the model and identifying assumptions.

peripheral yields remain elevated, economic activity falls, and prices rise. The ECB’s Transmission Protection Instrument launched in 2022 represents a step toward addressing such fragmentation risks. Nonetheless, the cross-border spillovers from sovereign stress underscore the critical importance of sound fiscal policies by national governments to maintain financial stability across the currency union.

Several promising avenues for future research emerge from our analysis. For instance, the identified shocks could be used together with structural models to conduct counterfactual policy analysis under weaker assumptions than pure model-based approaches ([McKay and Wolf, 2023](#)). Additionally, the identified shocks could help to recover the parameters of Taylor rules augmented with unconventional instruments following the approach proposed by [Barnichon and Mesters \(2020\)](#). We explore some of these extensions in ongoing work.

References

- Altavilla, Carlo, Luca Brugnolini, Refet S. Gürkaynak, Roberto Motto, and Giuseppe Rausa. 2019. "Measuring Euro Area Monetary Policy." *Journal of Monetary Economics* 108: 162-179.
- Andrade, Philippe and Filippo Ferroni. 2021. "Delphic and Odyssean Monetary Policy Shocks: Evidence from the Euro Area." *Journal of Monetary Economics* 117: 816-832.
- Antolín-Díaz, Juan and Juan F. Rubio-Ramírez. 2018. "Narrative Sign Restrictions for SVARs." *American Economic Review* 108(10): 2802-2829.
- Badinger, Harald and Stefan Schiman. 2023. "Measuring Monetary Policy Shocks for Small Open Economies: Evidence from a Structural Factor Model for Austria." *Journal of International Money and Finance* 137: 102910.
- Baek, In Choi and Yoonseok Lee. 2022. "The Local Projection Estimator is Consistent Under Weak Identification." *Journal of Econometrics* 230(2): 407-427.
- Barnichon, Regis, and Geert Mesters. 2020. "Identifying Modern Macro Equations with Old Shocks." *The Quarterly Journal of Economics* 135(4): 2255-2298.
- Bauer, Michael D., and Eric T. Swanson. 2023. "An Alternative Explanation for the 'Fed Information Effect'." *American Economic Review*, 113(3): 664–700.
- Bauer, Michael D., Aeimit Lakdawala, and Philippe Mueller. 2021. "Market-Based Monetary Policy Uncertainty." *NBER Working Paper* 29149.
- Caldara, Dario and Edward Herbst. 2019. "Monetary Policy, Real Activity, and Credit Spreads: Evidence from Bayesian Proxy SVARs." *American Economic Journal: Macroeconomics* 11(1): 157-192.
- Campbell, Jeffrey R., Charles L. Evans, Jonas D.M. Fisher, and Alejandro Justiniano. 2012. "Macroeconomic Effects of Federal Reserve Forward Guidance." *Brookings Papers on Economic Activity* 43(1): 1-80.

- Carriero, A., Clark, T. E., and Marcellino, M. (2016). Common drifting volatility in large Bayesian VARs. *Journal of Business & Economic Statistics*, 34(3):375–390.
- Cieslak, Anna. 2018. "Short-Rate Expectations and Unexpected Returns in Treasury Bonds." *Review of Financial Studies* 31(9): 3265-3306.
- Cloyne, James and Patrick Hürtgen. 2016. "The Macroeconomic Effects of Monetary Policy: A New Measure for the United Kingdom." *American Economic Journal: Macroeconomics* 8(4): 75-102.
- Ferreira, Leonardo N., Silvia Miranda-Agrippino, and Giovanni Ricco. 2025. "Bayesian Local Projections." *The Review of Economics and Statistics* 107(5): 1424-1438.
- Gertler, Mark and Peter Karadi. 2015. "Monetary Policy Surprises, Credit Costs, and Economic Activity." *American Economic Journal: Macroeconomics* 7(1): 44-76.
- Gürkaynak, Refet S., Brian Sack, and Eric T. Swanson. 2005. "Do Actions Speak Louder Than Words? The Response of Asset Prices to Monetary Policy Actions and Statements." *International Journal of Central Banking* 1(1): 55-93.
- Hóllo, Dániel, Manfred Kremer, and Marco Lo Duca. 2012. "CISS—A Composite Indicator of Systemic Stress in the Financial System." *ECB Working Paper* 1426.
- Istrefi, Klodiana, Florens Odendahl, and Giulia Sestieri. 2024. "High-Frequency Monetary Policy Shocks: Measurement and Narrative Identification." *Journal of Monetary Economics* 141: 103514.
- Jarociński, Marek. 2024. "Estimating the Fed's Unconventional Policy Shocks." *Journal of Monetary Economics* 144: 103543.
- Jarociński, Marek and Peter Karadi. 2020. "Deconstructing Monetary Policy Surprises—The Role of Information Shocks." *American Economic Journal: Macroeconomics* 12(2): 1-43.
- Jarociński, Marek and Peter Karadi. 2025. "What do r^* and Monetary Policy Shocks Tell Us about the Transmission of Monetary Policy?" *European Economic Review* 161: 104630.

Korobilis, Dimitris. 2022. "A New Algorithm for Structural Restrictions in Bayesian Vector Autoregressions." *European Economic Review* 148: 104241.

Kuttner, Kenneth N. 2001. "Monetary Policy Surprises and Interest Rates: Evidence from the Fed Funds Futures Market." *Journal of Monetary Economics* 47(3): 523-544.

Lopes, Hedibert Freitas and Mike West. 2004. "Bayesian Model Assessment in Factor Analysis." *Statistica Sinica* 14(1): 41-67.

McKay, Alisdair, and Christian K. Wolf. 2023. "What Can Time-Series Regressions Tell Us About Policy Counterfactuals?" *Econometrica* 91(5): 2045-2087.

Mertens, Karel and Morten O. Ravn. 2013. "The Dynamic Effects of Personal and Corporate Income Tax Changes in the United States." *American Economic Review* 103(4): 1212-1247.

Miranda-Agrippino, Silvia and Giovanni Ricco. 2021. "The Transmission of Monetary Policy Shocks." *American Economic Journal: Macroeconomics* 13(3): 74-107.

Miranda-Agrippino, S. and Ricco, G. (2023), "Identification with External Instruments in Structural VARs," *Journal of Monetary Economics*, 135, 1–19.

Montiel Olea, José Luis, Mikkel Plagborg-Møller, Eric Qian, and Christian K. Wolf. 2025. "Local Projections or VARs? A Primer for Macroeconomists." *Working Paper*, January 23.

Motto, Roberto and Kerem Özen. 2022. "Market-Stabilization QE." *ECB Working Paper* 2640.

Nakamura, Emi and Jón Steinsson. 2018. "High-Frequency Identification of Monetary Non-Neutrality: The Information Effect." *The Quarterly Journal of Economics* 133(3): 1283-1330.

Ramey, Valerie A. 2016. "Macroeconomic Shocks and Their Propagation." *Handbook of Macroeconomics* 2: 71-162.

Ricco, Giovanni, Alessandro Calza, and Tommaso Monacelli. 2025. "Monetary Policy, Information, and Country Risk Shocks in the Euro Area." *Journal of International Economics* 152: 103917.

Romer, Christina D. and David H. Romer. 1989. "Does Monetary Policy Matter? A New Test in the Spirit of Friedman and Schwartz." *NBER Macroeconomics Annual* 4: 121-170.

Romer, Christina D. and David H. Romer. 2004. "A New Measure of Monetary Shocks: Derivation and Implications." *American Economic Review* 94(4): 1055-1084.

Schmeling, Maik, Andreas Schrimpf, and Sigurd A.M. Steffensen. 2022. "Monetary policy expectation errors." *Journal of Financial Economics* 146(3): 841-858.

Stock, James H. and Mark W. Watson. 2012. "Disentangling the Channels of the 2007-09 Recession." *Brookings Papers on Economic Activity* 42(1): 81-135.

Swanson, Eric T. 2021. "Measuring the Effects of Federal Reserve Forward Guidance and Asset Purchases on Financial Markets." *Journal of Monetary Economics* 118: 32-53.

Swanson, Eric T. 2024. "The Macroeconomic Effects of Federal Reserve Unconventional Monetary Policy." *Journal of Monetary Economics* 144: 103540.

A Posterior Distributions

A.1 High-Frequency Model Posteriors

We employ a Gibbs sampling procedure to generate draws from the posterior distributions. The high-frequency model is:

$$\mathbf{y}_t = \boldsymbol{\Lambda} \boldsymbol{\epsilon}_t + \mathbf{B} \mathbf{x}_t + \mathbf{v}_t \quad (19)$$

$$\boldsymbol{\epsilon}_t \sim \mathcal{N}(\mathbf{0}, \boldsymbol{\Sigma}_{s_\epsilon}^\epsilon), \quad \mathbf{v}_t \sim \mathcal{N}(\mathbf{0}, \boldsymbol{\Sigma}_{s_v}^v), \quad s_\epsilon, s_v \in \{\text{low, high}\} \quad (20)$$

where the notation follows that presented in the main text.

Each element Λ_{ij} of the loadings matrix is sampled following Equation (8). The posterior for the structural shocks is given by:

$$\boldsymbol{\epsilon}_t | \cdot \sim \mathcal{N}(\bar{\boldsymbol{\mu}}_t, \bar{\boldsymbol{\Sigma}}_t) \quad (21)$$

$$\bar{\boldsymbol{\Sigma}}_t = \left(\boldsymbol{\Sigma}_{\epsilon, s_\epsilon(t)}^{-1} + \boldsymbol{\Lambda}' \mathbf{R}_t^{-1} \boldsymbol{\Lambda} \right)^{-1} \quad (22)$$

$$\bar{\boldsymbol{\mu}}_t = \bar{\boldsymbol{\Sigma}}_t \boldsymbol{\Lambda}' \mathbf{R}_t^{-1} \tilde{\mathbf{y}}_t \quad (23)$$

where $\boldsymbol{\Sigma}_{\epsilon, s_\epsilon(t)}$ denotes the regime-specific factor covariance matrix with diagonal elements $\sigma_{k, s_{\epsilon, k}(t)}^2$ for $k = 1, \dots, K$, \mathbf{R}_t is the diagonal matrix of idiosyncratic variances at time t , and $\tilde{\mathbf{y}}_t = \mathbf{y}_t - \mathbf{B} \mathbf{x}_t$.

For each factor k , the variance regime indicator $S_{tk} \in \{1(\text{low}), 2(\text{high})\}$ at time t is sampled from its posterior. Specifically, let $\sigma_{k,1}^2$ and $\sigma_{k,2}^2$ denote the low and high variances, then the posterior probability that $S_{tk} = 1$ is:

$$\Pr(S_{tk} = 1 | \cdot) = \frac{\pi_{1k} \times \phi(\epsilon_{tk}; 0, \sigma_{k,1}^2)}{\pi_{1k} \times \phi(\epsilon_{tk}; 0, \sigma_{k,1}^2) + (1 - \pi_{1k}) \times \phi(\epsilon_{tk}; 0, \sigma_{k,2}^2)} \quad (24)$$

where $\phi(\cdot; \mu, \sigma^2)$ denotes the normal density with mean μ and variance σ^2 , and π_{1k} is the probability factor k is in the low variance state. The latter is given by:

$$\pi_{1k} | \cdot \sim \text{Beta}(\underline{a}_\pi + N_{1k}, \underline{b}_\pi + N_{2k}) \quad (25)$$

where $N_{1k} = \sum_{t=1}^T \mathbf{1}\{S_{tk} = 1\}$ and $N_{2k} = \sum_{t=1}^T \mathbf{1}\{S_{tk} = 2\}$ count observations in each state. We set $\underline{a}_\pi = 4.0$ and $\underline{b}_\pi = 1.0$.

For each factor k and variance state $s \in \{1, 2\}$, the variance parameters follow inverse gamma posteriors:

$$\sigma_{k,s}^2 | \cdot \sim \text{InverseGamma}(\bar{\alpha}_s, \bar{\beta}_s) \quad (26)$$

$$\bar{\alpha}_s = \frac{\underline{\alpha}_s + N_{sk}}{2} \quad (27)$$

$$\bar{\beta}_s = \frac{\underline{\beta}_s + \sum_{t:S_{tk}=s} \epsilon_{kt}^2}{2} \quad (28)$$

where N_{sk} counts observations of factor k in state s . We set $(\underline{\alpha}_1, \underline{\beta}_1) = (0.5, 0.5)$ for the low variance state and $(\underline{\alpha}_2, \underline{\beta}_2) = (0.5, 5.0)$ for the high variance state. After sampling, the states are reordered to ensure $\sigma_{k,1}^2 < \sigma_{k,2}^2$ by swapping variances and flipping state indicators if necessary.

During the factor selection phase described in Section 2.2, we use Bayesian LASSO shrinkage with factor-specific hierarchical priors on the loadings to determine the dimension K of $\boldsymbol{\epsilon}_t$. Under this prior, each loading Λ_{ij} has a conditional Laplace prior with precision parameter ψ_{ij} that depends on a factor-specific rate parameter δ_j . The precision parameter follows a gamma posterior:

$$\psi_{ij} | \cdot \sim \text{Gamma}(\bar{\alpha}_\psi, \bar{\beta}_\psi) \quad (29)$$

$$\bar{\alpha}_\psi = \underline{\alpha}_\psi + \frac{1}{2} \quad (30)$$

$$\bar{\beta}_\psi = \left(\delta_j + \frac{\Lambda_{ij}^2}{2} \right)^{-1} \quad (31)$$

where we set $\underline{\alpha}_\psi = 1.0$. The factor-specific rate parameter δ_j has posterior:

$$\delta_j | \cdot \sim \text{Gamma}(\bar{\alpha}_\delta, \bar{\beta}_\delta) \quad (32)$$

$$\bar{\alpha}_\delta = \underline{a}_\lambda + N \quad (33)$$

$$\bar{\beta}_\delta = \left(\underline{b}_\lambda^{-1} + \sum_{i=1}^N \psi_{ij} \right)^{-1} \quad (34)$$

where we set $\underline{a}_\lambda = 0.25$ and $\underline{b}_\lambda = 0.25$ for moderate shrinkage. Once K is determined, we switch to Normal priors without shrinkage for the main estimation.

For each row i of the coefficient matrix \mathbf{B} corresponding to control variables, let $\hat{y}_{it} = y_{it} - \sum_k \Lambda_{ik} \epsilon_{kt}$ denote the residual after removing the contribution of structural shocks. The posterior for $\mathbf{B}_{i,\cdot}$ is given by:

$$\mathbf{B}_{i,\cdot} | \cdot \sim \mathcal{N}(\bar{\mu}_{\mathbf{B}_{i,\cdot}}, \bar{\Sigma}_{\mathbf{B}_{i,\cdot}}) \quad (35)$$

$$\bar{\Sigma}_{\mathbf{B}_{i,\cdot}} = \left(\underline{\Omega}_B + \sum_{t=1}^T \frac{\mathbf{x}_t \mathbf{x}'_t}{\sigma_{i,s_v(t)}^v} \right)^{-1} \quad (36)$$

$$\bar{\mu}_{\mathbf{B}_{i,\cdot}} = \bar{\Sigma}_{\mathbf{B}_{i,\cdot}} \left(\underline{\Omega}_B \underline{\mu}_B + \sum_{t=1}^T \frac{\mathbf{x}_t \hat{y}_{it}}{\sigma_{i,s_v(t)}^v} \right) \quad (37)$$

where we set $\underline{\Omega}_B = 10 \times \mathbf{I}_M$ and $\underline{\mu}_{B=0}$.

Under the mixture specification for idiosyncratic variances, for each asset i and time t , the variance regime indicator $S_{r,it} \in \{1(\text{low}), 2(\text{high})\}$ is sampled from its posterior analogously to the factor regime indicators. Let $r_{i,1}$ and $r_{i,2}$ denote the low and high variances for asset i , then the posterior probability that $S_{r,it} = 1$ is given by:

$$\Pr(S_{r,it} = 1 | \cdot) = \frac{\pi_{r,i} \times \phi(v_{it}; 0, r_{i,1})}{\pi_{r,i} \times \phi(v_{it}; 0, r_{i,1}) + (1 - \pi_{r,i}) \times \phi(v_{it}; 0, r_{i,2})} \quad (38)$$

where $v_{it} = y_{it} - \sum_k \Lambda_{ik} \epsilon_{kt} - \sum_m B_{im} x_{mt}$ is the idiosyncratic error and $\pi_{r,i}$ is the probability of being in the low variance state. The state probability $\pi_{r,i}$ and variance parameters $r_{i,1}$ and $r_{i,2}$ are sampled from beta and inverse gamma posteriors analogously to the factor variances, with states reordered after sampling to ensure $r_{i,1} < r_{i,2}$.

A.2 Bayesian VAR-DL Posteriors

We employ a Gibbs sampling procedure to generate draws from the posterior distributions. The VAR-DL model is:

$$\mathbf{y}_t = \sum_{l=1}^p \Phi_l \mathbf{y}_{t-l} + \sum_{j=0}^q \Psi_j \mathbf{m}_{t-j} + \mathbf{v}_t \quad (39)$$

$$\mathbf{v}_t \sim \mathcal{N}(\mathbf{0}, \Sigma_t), \quad \Sigma_t = e^{h_t} \Sigma, \quad h_t = \rho_h h_{t-1} + u_t^h, \quad u_t^h \sim \mathcal{N}(0, \sigma_h^2) \quad (40)$$

where the notation follows that presented in the main text.

We volatility-weight the data for sampling. Let $\sqrt{w_t} = \exp(h_t/2)$ denote the volatility scaling factor. The weighted variables are $\mathbf{y}_{t,w} = \mathbf{y}_t/\sqrt{w_t}$, and similarly for the lagged endogenous variables and distributed lag regressors.

For each equation i , let ϕ_i denote the stacked vector of autoregressive coefficients and $\psi_i = [\psi_{i,0}, \psi_{i,1}, \dots, \psi_{i,q}]'$ denote the $(q+1) \times 1$ vector of distributed lag coefficients on the monetary policy shock. The posterior for ϕ_i follows from conjugate normal-normal updating under Minnesota priors:

$$\phi_i | \cdot \sim \mathcal{N}(\bar{\mu}_{\phi_i}, \bar{\Sigma}_{\phi_i}) \quad (41)$$

$$\bar{\Sigma}_{\phi_i} = \left(\underline{\Omega}_{\phi_i} + \sigma_{ii}^{-1} \sum_{t=1}^T \mathbf{Y}_{t,w} \mathbf{Y}'_{t,w} \right)^{-1} \quad (42)$$

$$\bar{\mu}_{\phi_i} = \bar{\Sigma}_{\phi_i} \left(\underline{\Omega}_{\phi_i} \underline{\mu}_{\phi_i} + \sigma_{ii}^{-1} \sum_{t=1}^T \mathbf{Y}_{t,w} y_{i,t,w}^* \right) \quad (43)$$

where $\mathbf{Y}_{t,w} = [\mathbf{y}'_{t-1,w}, \mathbf{y}'_{t-2,w}, \dots, \mathbf{y}'_{t-p,w}]'$ is the stacked vector of lagged endogenous variables, $y_{i,t,w}^* = y_{i,t,w} - \sum_{j=0}^q \psi_{i,j} m_{t-j,w}$ is the residualized dependent variable, σ_{ii} is the i -th diagonal element of Σ , and $\underline{\Omega}_{\phi_i}$ is the Minnesota prior precision matrix. The Minnesota prior mean $\underline{\mu}_{\phi_i}$ for asset i is a vector of zeros with a single entry equal to 1 for the first own lag of variable i . The Minnesota prior variances are $\text{Var}(\phi_{i,i}^{(l)}) = (\lambda_1/l^{\lambda_3})^2$ for own lags and $\text{Var}(\phi_{i,j}^{(l)}) = (\sigma_i/\sigma_j) \cdot (\lambda_1 \lambda_2/l^{\lambda_3})^2$ for cross-lags, where λ_1 controls overall tightness, λ_2 controls cross-lag shrinkage, and λ_3 controls lag decay. We set $\lambda_1 = 0.2$, $\lambda_2 = 0.5$, and $\lambda_3 = 1.0$.

The posterior for ψ_i depends on the shrinkage specification. Under both specifications, the posterior takes the form:

$$\psi_i | \cdot \sim \mathcal{N}(\bar{\mu}_{\psi_i}, \bar{\Sigma}_{\psi_i}) \quad (44)$$

$$\bar{\Sigma}_{\psi_i} = \left(\underline{\Omega}_{\psi_i} + \sigma_{ii}^{-1} \sum_{t=1}^T \mathbf{M}_{t,w} \mathbf{M}'_{t,w} \right)^{-1} \quad (45)$$

$$\bar{\mu}_{\psi_i} = \bar{\Sigma}_{\psi_i} \left(\underline{\Omega}_{\psi_i} \underline{\mu}_{\psi_i} + \sigma_{ii}^{-1} \sum_{t=1}^T \mathbf{M}_{t,w} \tilde{y}_{i,t,w} \right) \quad (46)$$

where $\mathbf{M}_{t,w} = [m_{t,w}, m_{t-1,w}, \dots, m_{t-q,w}]'$ is the stacked vector of current and lagged shocks, and $\tilde{y}_{i,t,w} = y_{i,t,w} - \sum_{l=1}^p \phi'_{i,l} \mathbf{y}_{t-l,w}$ is the residualized dependent variable after removing the contribution of autoregressive lags. When sign restrictions are imposed, we sample from the corresponding truncated normal distribution. If dynamic sign restrictions are used, we use an accept/reject algorithm to sample from the posterior conditional on such restrictions. The prior specification $(\underline{\Omega}_{\psi_i}, \underline{\mu}_{\psi_i})$ differs between the two shrinkage approaches.

Under the difference penalty specification, we impose the Bayesian ridge prior described in Equation (16) of the main text, which penalizes d -th order differences in the impulse-response coefficients. This specification sets $\underline{\Omega}_{\psi_i} = \mathbf{I}_{q+1} + \lambda_i^d \mathbf{P}$ and $\underline{\mu}_{\psi_i} = \mathbf{0}$, where \mathbf{P} is the penalty matrix defined in Equation (17).

The smoothing parameter λ_i^d is estimated from the data using a hierarchical prior $\lambda_i^d \sim \text{Gamma}(\underline{\alpha}_{\lambda^d}, \underline{\beta}_{\lambda^d})$, where we set $\underline{\alpha}_{\lambda^d} = 1.0$ and $\underline{\beta}_{\lambda^d} = 0.1$. The conditional posterior for λ_i^d is given by Equation (18).

Under the polynomial shrinkage specification, we express the distributed lag coefficients as $\psi_i = \mathbf{Z}\gamma_i$, where \mathbf{Z} is the $(q+1) \times (K_\gamma + 1)$ polynomial basis matrix with elements $Z_{j,k} = j^k$ for lag j and polynomial order $k \in \{0, 1, \dots, K_\gamma\}$, and γ_i are the polynomial coefficients. The posterior for γ_i is:

$$\gamma_i | \cdot \sim \mathcal{N}(\bar{\mu}_{\gamma_i}, \bar{\Sigma}_{\gamma_i}) \quad (47)$$

$$\bar{\Sigma}_{\gamma_i} = \left(\underline{\Omega}_{\gamma_i} + \frac{\lambda_i^p}{\sigma_{ii}} \mathbf{Z}' \mathbf{Z} \right)^{-1} \quad (48)$$

$$\bar{\mu}_{\gamma_i} = \bar{\Sigma}_{\gamma_i} \left(\underline{\Omega}_{\gamma_i} \underline{\mu}_{\gamma_i} + \frac{\lambda_i^p}{\sigma_{ii}} \mathbf{Z}' \psi_i \right) \quad (49)$$

where $\underline{\mu}_{\gamma_i} = \mathbf{0}$ and $\underline{\Omega}_{\gamma_i} = 0.01 \times \mathbf{I}_{K_\gamma+1}$. Under this specification, the priors for the distributed lag coefficients are given by $\underline{\mu}_{\psi_i} = \mathbf{Z}\gamma_i$ and $\underline{\Omega}_{\psi_i} = (\lambda_i^p / \sigma_{ii}) \mathbf{I}_{q+1}$. The shrinkage intensity

parameter λ_i^p has a posterior defined by:

$$\lambda_i^p | \cdot \sim \text{Gamma}(\bar{\alpha}_p, \bar{\beta}_p) \quad (50)$$

$$\bar{\alpha}_p = \underline{\alpha}_p + \frac{q+1}{2} \quad (51)$$

$$\bar{\beta}_p = \underline{\beta}_p + \frac{1}{2\sigma_{ii}} \sum_{j=0}^q (\psi_{i,j} - [\mathbf{Z}\boldsymbol{\gamma}_i]_j)^2 \quad (52)$$

where we set $\underline{\alpha}_p = 0.1$ and $\underline{\beta}_p = 0.1$.

The residual covariance matrix $\boldsymbol{\Sigma}$ follows an inverse Wishart posterior. Let $\mathbf{u}_{t,w} = \mathbf{y}_{t,w} - \sum_{l=1}^p \boldsymbol{\Phi}_l \mathbf{y}_{t-l,w} - \sum_{j=0}^q \boldsymbol{\Psi}_j \mathbf{m}_{t-j,w}$ denote the volatility-weighted residuals. The posterior is:

$$\boldsymbol{\Sigma} | \cdot \sim \text{InverseWishart}(\bar{\nu}, \bar{\mathbf{S}}) \quad (53)$$

$$\bar{\nu} = \underline{\nu} + T \quad (54)$$

$$\bar{\mathbf{S}} = \underline{\mathbf{S}} + \sum_{t=1}^T \mathbf{u}_{t,w} \mathbf{u}_{t,w}' \quad (55)$$

where $\underline{\nu} = N + 2$ and $\underline{\mathbf{S}} = \text{diag}(\hat{\sigma}_1^2, \dots, \hat{\sigma}_N^2)$ with $\hat{\sigma}_i^2$ estimated from univariate AR(p) regressions.

The common stochastic volatility states $\mathbf{h} = (h_1, \dots, h_T)'$ are sampled using a precision-based algorithm following [Carriero et al. \(2016\)](#). Let $\mathbf{s}^2 = (s_1^2, \dots, s_T^2)'$ denote the vector of squared standardized residuals, where $s_t^2 = \mathbf{u}_t' \boldsymbol{\Sigma}^{-1} \mathbf{u}_t$.

We begin by constructing the precision matrix for the AR(1) prior. Let \mathbf{H}_ρ denote the $T \times T$ whitening transformation matrix with ones on the main diagonal and $-\rho_h$ on the first subdiagonal, and let $\boldsymbol{\Omega}_h$ be the diagonal precision matrix for the innovations with elements $\omega_{11} = (1 - \rho_h^2)/\sigma_h^2$ and $\omega_{tt} = 1/\sigma_h^2$ for $t > 1$. The prior precision is given by $\mathbf{H}_\rho' \boldsymbol{\Omega}_h \mathbf{H}_\rho$.

Since the conditional posterior $p(\mathbf{h} | \cdot)$ is non-Gaussian due to the exponential form of the likelihood, we locate its mode \mathbf{h}^* using Newton-Raphson iterations. At each iteration, we solve:

$$\mathbf{K}_h \mathbf{h}^{\text{new}} = \mathbf{f}_h + \mathbf{G}_h \mathbf{h}^t \quad (56)$$

where \mathbf{f}_h is the gradient of the log-likelihood with elements $f_{ht} = -N/2 + s_t^2 e^{-h_t}/2$, $\mathbf{G}_h =$

$\text{diag}(s_1^2 e^{-h_1}/2, \dots, s_T^2 e^{-h_T}/2)$ is the diagonal negative Hessian, and $\mathbf{K}_h = \mathbf{H}'_\rho \boldsymbol{\Omega}_h \mathbf{H}_\rho + \mathbf{G}_h$ combines the prior precision with the likelihood curvature. Convergence yields the posterior mode \mathbf{h}^* and the matrix \mathbf{K}_h .

To sample from the exact posterior, we employ a hybrid accept-reject Metropolis-Hastings algorithm. We first generate a high-quality proposal \mathbf{h}^c via accept-reject sampling from the Gaussian approximation $\mathcal{N}(\mathbf{h}^*, \mathbf{K}_h^{-1})$. We repeatedly draw candidates until one satisfies:

$$\alpha^{AR}(\mathbf{h}^c) = -\frac{1}{2}\mathbf{h}^{c'} \mathbf{H}'_\rho \boldsymbol{\Omega}_h \mathbf{H}_\rho \mathbf{h}^c - \frac{N}{2} \sum_{t=1}^T h_t^c - \frac{1}{2} \sum_{t=1}^T s_t^2 e^{-h_t^c} + \frac{1}{2} (\mathbf{h}^c - \mathbf{h}^*)' \mathbf{K}_h (\mathbf{h}^c - \mathbf{h}^*) - \log c > \log U \quad (57)$$

where c is a control constant and $U \sim \text{Uniform}(0, 1)$. We then treat \mathbf{h}^c as a proposal in a Metropolis-Hastings step, accepting the move from the current state \mathbf{h} to \mathbf{h}^c with probability $\min\{1, \exp(\alpha^{MH})\}$, where $\alpha^{MH} = \alpha^{AR}(\mathbf{h}^c) - \alpha^{AR}(\mathbf{h})$. This two-stage procedure ensures we sample from the exact posterior while maintaining computational efficiency. For numerical stability, we exploit the tridiagonal structure of \mathbf{K}_h using banded Cholesky decompositions.

The persistence parameter ρ_h is sampled via Metropolis-Hastings with a Gaussian proposal centered at the posterior mode from a simplified regression of h_t on h_{t-1} . The proposal has precision $K_\rho = \underline{\sigma}_\rho^{-2} + \sum_{t=2}^T h_{t-1}^2 / \sigma_h^2$ and mean $\hat{\rho}_h = K_\rho^{-1} (\underline{\sigma}_\rho^{-2} \underline{\rho}_h + \sum_{t=2}^T h_{t-1} h_t / \sigma_h^2)$, where $\underline{\rho}_h$ and $\underline{\sigma}_\rho^2$ are prior hyperparameters. We set $\underline{\rho}_h = 0.9$ and $\underline{\sigma}_\rho^2 = 0.1$. The acceptance ratio includes correction terms for the stationarity constraint and the first observation:

$$\log \alpha(\rho_{\text{cand}}, \rho_h) = \frac{1}{2} \log \frac{1 - \rho_{\text{cand}}^2}{1 - \rho_h^2} - \frac{1}{2\sigma_h^2} [(1 - \rho_{\text{cand}}^2)h_1^2 - (1 - \rho_h^2)h_1^2] \quad (58)$$

The innovation variance σ_h^2 follows an inverse gamma posterior:

$$\sigma_h^2 | \cdot \sim \text{InverseGamma}(\bar{\alpha}_h, \bar{\beta}_h) \quad (59)$$

$$\bar{\alpha}_h = \underline{\alpha}_h + \frac{T}{2} \quad (60)$$

$$\bar{\beta}_h = \underline{\beta}_h + \frac{1}{2} \left[\sum_{t=2}^T (h_t - \rho_h h_{t-1})^2 + (1 - \rho_h^2)h_1^2 \right] \quad (61)$$

where we set $\underline{\alpha}_h = 5.0$ and $\underline{\beta}_h = 0.04$.

Finally, we sample the latent monetary policy shocks \mathbf{m}_t at each MCMC iteration from the posterior draws obtained from the high-frequency Bayesian factor model, thereby propagating estimation uncertainty from the high-frequency identification stage to the macroeconomic analysis.

B Additional Figures

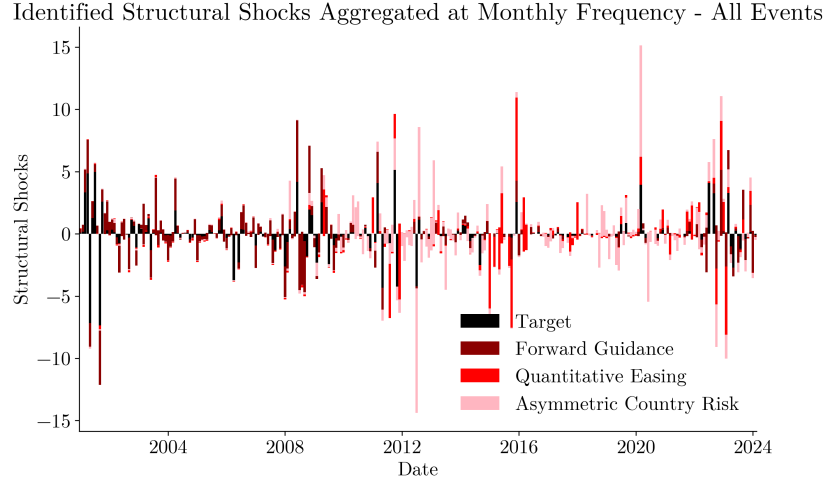


Figure 1: Identified Structural Shocks Aggregated at Monthly Frequency

Notes: Figure plots the identified high-frequency monetary policy shocks aggregated at monthly frequency. The shocks are obtained from the high-frequency Bayesian factor model described in Section 2.1. Each bar represents the sum of shocks within a given month across all policy events. Sample covers the period 2001M1-2024M2.

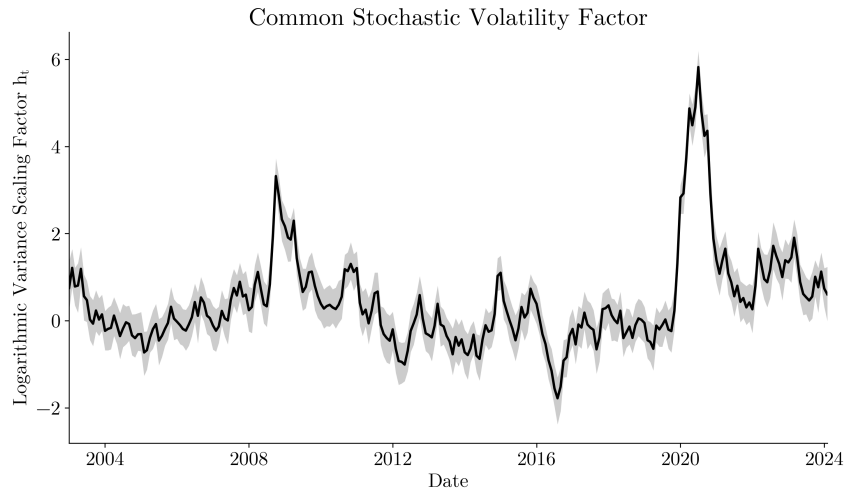


Figure 2: Common Stochastic Volatility Factor

Notes: Figure plots the estimated common stochastic volatility factor h_t from the Bayesian VAR-DL model described in Section 4.1. The solid black line shows the posterior median of the logarithmic variance scaling factor with shaded 68% HPD bands. Sample covers the period 2001M1-2024M2.